GSA Data Repository 2017168

Suan et al., 2017, Subtropical climate conditions and mangrove growth in Arctic Siberia during the early Eocene: Geology, doi:10.1130/G38547.1.

1. Material and methods.

1.1. Sample localities

The samples for this study were collected in 2011 during the CASE 13 expedition from two Eocene sedimentary successions cropping out on the New Siberian Islands. The New Siberian Islands archipelago is located on the Laptev Sea shelf, north of the Lena River Delta. The islands represent the emerged basement portions of a complex rift system that has affected the Siberian shelf in the continuation of the Eurasian Basin since the Late Cretaceous. This system constitutes today a diffuse plate boundary between Eurasia and North America. The studied series were deposited unconformably on a folded Mesozoic and Paleozoic substratum and were preserved within hanging-walls of N-S normal faults related to rifting (Fig. DR1). The Cenozoic series is mainly composed of clays and silts interbedded with sands and brown coal seams that were deposited in a continental setting (Kos'ko and Korago, 2009).

Tectonic reconstructions indicate that the position of the New Siberian Islands with respect to Eurasia has not been drastically modified since Eocene times. The finite amount of stretching due to the opening of the Ust'Lena Rift, and the Anisin and New Siberian Basins since the Paleocene is estimated about 580 km to 640 km in E-W direction (Franke and Hinz, 2009; Gaina et al., 2002). Taking into account a maximum of 400 km eastward displacement of the New Siberian Islands relative to Siberia since 50 Ma (Franke and Hinz, 2009), and a paleopole at 81.6°N, 238.8°E for East Asia between 50-60 Ma (Cogné et al., 2013), the

considered sites were situated at a paleolatitude of at least 72.3°N or higher. Such estimates are in line with those given for the NSI by the paleolatitude calculator computed by van Hinsbergen et al. (2015), which range between 74.5 and 85.7°N at 50 Ma for their three different paleomagnetic reference frames.

Twenty-six samples were collected from the Anjou Formation (Fig. DR2), located on the northern part of Faddeevsky Island (N76°06’23,3" / E141°49’01,7"). The measured section comprises a 35 m-thick succession that can be subdivided into three separate lithological units (Fig. DR2). The lowermost Unit If consists of massive, up to 1 m thick lignite seams that contain abundant amber pebbles and are intercalated with 10-20 centimeters brownish-gray clay beds rich in wood debris. The overlying Unit IIf mainly consists of gray, unconsolidated, silty to sandy clays rich in wood particles and containing several horizons with siderite nodules; the lower part of Unit IIf shows meter-scale trough cross-bedding. The sampling density of this unit was lower compared to other units due to extensive ice cover during the expedition. Unit IIIf is dominated by lignite seams rich in amber particles and interbedded with unconsolidated, fine-grained clayey silty to sand beds containing common wood debris, and a dense network of thin (diameter ~2cm) vertical root-like structures (Fig. DR2C). The density and vertical arrangement of these structures resemble that of pneumatophores, consistent with the occurrence of *Avicennia* and *Glyptostrobus*-*Taxodium*-type pollen grains in the same section.

Sixteen additional samples were collected from the Paleogene (Fig. 1) of the eastern part of Belkovsky Island (N75°30’16,7" / E135°59’07,4"). The measured section is 2.4 m thick and consists of light greenish-gray, unconsolidated fine-grained and clayey sands interrupted by a ~10 cm-thick bed of dark gray silt at 0.65 m and a coarser conglomerate horizon containing rounded pebbles at 1.8 m (Fig. DR2). The lower part of the section shows meter-scale, low-angle trough cross-bedding (Fig. DR2).

1.2. Methods.

1.2.1 Palynology.

For palynological analyses, one to five grams of sediments were physico-chemically processed, starting with acid digestion by HCl, HF, and HCl again, followed by concentration in $ZnCl_2$ and sieving at 10 µm. An aliquot of 50 µl of residue was diluted in glycerol, allowing the rotation of palynomorphs and their examination on all sides (Cour, 1974), and examined under a light microscope at magnification x200. Identifications were realized at magnification x1000. Pollen grains from the Belkovsky and Faddeevsky islands are exceptionally well-preserved, a condition that allows a detailed examination of their morphological characters and their botanical identification after comparison with material from modern pollen databases. More than 100 pollen grains were counted per sample in addition to those of *Pinus*, as this genus can be over-represented in coastal deltaic sediments (Beaudouin et al., 2005). The raw counts are presented in Tables S1 and S2.

1.2.2. Paleoclimate.

The effort in pollen identification and counting allows the "Climatic Amplitude Method" to be used for reconstructing climate conditions during the deposition of the Faddeevsky and Belkovsky Island successions (Fauquette et al., 1998). The estimated mean annual temperatures (MAT), mean annual precipitation (MAP), mean temperatures of the coldest (MTC) and warmest (MTW) months concern the low-altitude vegetation because meso-microthermal (with *Cathaya* living today in altitude in subtropical China) and microthermal taxa have been excluded from the process to avoid a cold bias linked to transport from higher elevations. The excluded taxa were defined on the base of the modern vegetation distribution. Indeed, vegetation types described for the early Eocene in the New Siberian Islands are found today in Southeastern China from around 25 to 30°N and 110 to 120°E (Hou, 1983). In this

region, the vertical distribution of the vegetation is characterized, from the base to the top of the massifs (for instance at Taibai Shan in the Tsinling Massif, Shaanxi, and Taba Shan, eastern Sichuan or Hua Ping, Guangxi), by the evergreen broad-leaved forest, mixed evergreen and deciduous (*Betula*, *Acer*) broad-leaved forest, *Cathaya*/*Tsuga* forest, *Picea*/*Abies* forest and high mountain meadows (Wang, 1961; Hou, 1983). The estimates for each climatic parameter are given as an interval (minimum and maximum values of the parameter) and a Most Likely Value (MLV) corresponding to a weighted mean, a statistical calculation tested on modern pollen data that has provided reliable results (for more details, see Fauquette et al., 1998).

1.2.3. Palynofacies.

Palynofacies components were determined using standard procedures (Tyson, 1995) involving carbonate and silicate removal through HCl-HF digestion. Neither oxidation nor ultrasonic probe was carried out to avoid destruction of some organic particles. The residue was separated into two fractions. One was directly mounted on glass microscope slides and the other after sieving through a 10 μm sieve. The relative amounts (surface per field of view) of the following organic particle categories were determined using a Zeiss Axioskop 40 microscope under different illumination modes based on the classification of ref (Whitaker, 1984): i) phytoclasts, which correspond to all land plant remains that have been divided into subgroups represented by semi-opaque (palynomacerals 1 and 2) and opaque debris (palynomaceral 4), which include all ligneous and woody fragments, and translucent plant debris (palynomaceral 3), such as fragments of leaf cuticles and epidermis; ii) land-derived pollen grains and spores (sporomorphs); iii) *Botryococcus* algae; iv) Amorphous Organic Matter (AOM), which includes flaky orange to dark brown-colored organic components without visible biological structure under light microscopy; v) amber particles. Fluorescence microscopy was used to characterize the preservation state of AOM and identify

Botryococcus algae. The relative variations in abundance of all these particles in the study sites are presented in the Figure DR3 and Table DR3.

1.2.4. Organic and stable isotope geochemistry.

Total organic carbon content, thermal maturation and source of the organic matter were determined using a Rock-Eval Instrument in standard conditions (Behar et al., 2001). The organic carbon-isotope composition ($\delta^{13}C$), total nitrogen (TN) and total sulfur (TS) measurements were determined for all bulk samples. The same parameters were also determined for an aliquot of more than 50 amber particles and a bulk wood sample collected along the Faddeevsky succession for comparisons with bulk organic matter and chronostratigraphy (see section 2 below). Between 0.2 to 1 mg of fully decarbonated sediment powder was weighted into tin capsules and placed in a Pyrocube® elemental analyzer connected to Elementar Isoprime® isotope-ratio mass spectrometer in continuous flow. Each analytical run contained four sets of two standards (NBS 127 and aspartic acid) to monitor analytical precision and accuracy. All samples were duplicated and the carbon isotope results are reported relative to the 'Vienna Peedee belemnite' (VPDB) in delta notation $\delta^{13}C$. The precision was better than 0.15‰ for carbon isotope ratios and 2% of the reported value for both TOC and TS contents of the carbonate-free fraction.

1.2.5. Whole-rock and clay mineralogy.

The analysis of whole-rock and clay mineralogy was determined using X-ray diffraction (XRD). X-ray diffractograms were obtained using a D2 Brucker diffractometer equipped with a LynxEye detector, with CuKα radiation and NI filter. Measurement parameters were as follows: 2 2.5 to 75°(2θ) and 2.5 to 35° (2θ) for whole-rock and clay mineralogy analysis, respectively. Step measurements were of 0.02° (2θ) each 0.2 s. The samples for clay mineral analysis were prepared using the analytical procedure of Holtzapffel (1985). Identification of minerals was made according to the position of the (001) series of basal reflections. For clay

minerals, three X-ray diagrams, respectively obtained with non-treated, glycolated, and heated (450 °C, 4 h) preparations (Brown et al., 1980; Moore and Reynolds, 1989) were analyzed. Semiquantitative evaluations are based on the peak areas estimated using the Macdiff software. Areas were summed to 100%, the relative error being 5% (Holtzapffel, 1985). Organic-rich samples (TOC>10%) were treated using hydrogen peroxide (H_2O_2). The relative variations in abundance of all whole-rock and clay minerals are presented in the Figure DR3 and Table DR3.

2. Age of the successions.

2.1. Faddeevsky Island.

Previous palynological and lithological correlation indicate an Eocene age for the Anjou Formation on Faddeevsky Island (Kos'ko and Trufanov, 2002). Our data show that three levels in the lower part of the measured succession contain abundant dinoflagellate cysts, >90% of which belong to *Apectodinium parvum* (Fig S4). We interpret this *Apectodinium*-dominated interval as the *Apectodinium* acme marking the onset of the Paleocene-Eocene Thermal Maximum (PETM; early Ypresian) on a global scale (Bujak and Brinkhuis, 1998; Crouch et al., 2003; Crouch et al., 2001; Iakovleva, 2016; Sluijs et al., 2008). *Apectodinium parvum* has a slightly longer range in Western Siberia than *Axiodinium* (*Apectodinium*) *augustum*, a species diagnostic of the Paleocene-Eocene Thermal Maximum (PETM; early Ypresian) (Sluijs et al., 2006; Williams et al., 2015), but is restricted to the lower part of the lower Eocene (Iakovleva and Kulkova, 2003). The absence of *Axiodinium* (*Apectodinium*) in the studied assemblage is probably due to the coastal position of the studied section. In addition, the strata where the *Apectodinium* acme occurs at Faddeevsky show a ~2.5‰ organic carbon-isotope ($\delta^{13}C_{TOC}$) carbon-isotope excursion (CIE) comparable to that recorded during the PETM in marine records (Fig. DR5). Our $\delta^{13}C_{TOC}$ records from this locality do no

show correlation with the abundance of specific organic components deduced from palynofacies and geochemical analyses, and thus most likely reflect genuine carbon-cycle perturbations (see section 4 of this SI). Given the co-occurrence of the *Apctodinium* acme and this CIE, we are confident in attributing the interval between 1.85 m and 4.15 m at Faddeevsky to the PETM.

The second ~2‰ CIE recorded between 31 and 33 m show similarities with that recorded in many marine records and attributed to secondary hyperthermal events (Fig. DR5). Although lower sampling density in the middle part of the section limits detailed comparisons with lower Eocene marine $\delta^{13}C$ curves, we attribute this second CIE recorded at Faddeevsky (Fig. DR5) to the early Eocene thermal maximum (ETM) (Kirtland Turner et al., 2014). According to our correlation, the ~35 m thick succession would record ~2 Myr of coastal plain sedimentation (Fig. DR3). Such sedimentation rates are in line of average rates of 50 000 to 100 000 years per meter suggested for coal accumulation in passive margins (McCabe, 1990), which would result in a total duration comprised between 1.75 and 3.5 Myrs for the Faddeevsky succession. Such low rates of subsidence and accumulation are consistent with the limited thickness of Paleogene deposits in the New Siberian Islands (Kos'ko and Trufanov, 2002; Kos'ko and Korago, 2009).

2.2. Belkovsky Island.

The likelihood of the $\delta^{13}C_{TOC}$ curve reflects essentially changes in carbon-bearing elements (section 4 of this Supplement) precludes its use as a chemostratigraphic marker, particularly given the limited thickness of the measured section (~2 m). The palynological results provide further arguments for proposing an age assignment to the Belkovsky Island section, especially the absence of dinoflagellate cysts of the *Apectodinium* complex. From the climatic viewpoint, pollen data indicate slightly cooler conditions for the Belkovsky Island section

than for the Faddeevsky Island section. This section could thus precede or follow the PETM-ETM2 interval. The absence of primitive floral element in the pollen assemblage, such as components of the *Normapolles* - *Aquilapollenites* complexes, with uncertain link with any living angiosperm (Batten, 1981; Friis et al., 2006), rather supports a younger age than the Faddeevsky section and thus than the PETM-ETM2 interval. Abundant *Azolla* spores, also gathered with some sporangia, in several levels at Belkovsky Island (Table DR2) could possibly represent the massive *Azolla* blooms recorded in the central and western Arctic Ocean and in Norwegian-Greenland basins close to the Ypresian-Lutetian transition (ca. 49 Ma), and interpreted as a discharge of fresh waters in relation with cooler conditions (Barke et al., 2012; Brinkhuis et al., 2006; Moran et al., 2006). The free-floating, freshwater fern *Azolla* is however a long ranging-taxon, so that its occurrence in a coastal sites such as that of Belkovsky Island may simply represent a local bloom unrelated to the *Azolla* event. Therefore, correlation to the *Azolla* event awaits further confirmation and the Belkovsky Island section should be considered Ypresian-earliest Lutetian in age.

A recent study (Kuzmichev et al., 2013) based on palynology and plant macroremains gives a Late Eocene age for the base of the post-Paleozoic sequence of Belkovsky Island (their bed 1) and an Oligocene-Miocene age for the overlying strata. Comparison of our photographs of the section with those of this study (Fig. DR2, E, F, H) shows that our measured Unit Ib and IIb likely corresponds their bed 10 and base bed 11, respectively (0.2 m lignite seam at the base overlain by dark clayey sand above and terminated by top conglomerate). Based on the absence of 'thermophillous' elements in the pollen assemblages of their sample 1158/1 (roughly at the base of Unit IIb; Fig. DR2), these authors concluded that bed 11 is early Miocene in age. Our study however shows the occurrence of mega-mesotherms in this interval (Arecaceae, *Engelhardia*, *Glyptostrobus*-*Taxodium*-type, etc.) plus *Cathaya*, in similar abundance to that observed during the early Aquitanian in the

Northwestern Mediterranean (Bessedik, 1984). Difference in latitude makes impossible such pollen floras to be coeval and, as a consequence, allows discarding a Miocene age for these levels, which most likely formed during the beginning of the cooling phase following the Early Eocene Climatic Optimum

3. Environmental reconstructions based on pollen flora.

3.1. Methodological notes.

It is well known that type and degree of pollen identifications with respect to botanical nomenclature vary according to preservation of pollen grains and degree of specialization in morphology of pollen analysts. Pollen floras from high-latitude Paleogene deposits are not exceptions in this matter. They belong to two concepts using distinct approaches, respectively: i) a binomial nomenclature, generally based on a few, major morphological characters, which suggest identification at the species level; ii) a botanical nomenclature, based on detailed pollen morphology by comparison with modern pollen databases, more often restricted to the genus level.

Currently, most of the works on the high-latitude Paleogene follow a mixed approach referring (1) to botanical genera for some pollen very easy to identify, such as *Carya*, *Liquidambar*, *Alnus*, *Tilia*, etc., and (2) to binomial names for pollen grains requiring a detailed morphological examination (Frederiksen et al., 2002; Harrington et al., 2012; Kalkreuth et al., 1993; Kalkreuth et al., 1996; Ridgway et al., 1995). However, botanical identification of pollen grains at the family or genus level is becoming increasingly used by the community (Eldrett et al., 2009, 2014; Harrington et al., 2012; Liu and Basinger, 2000; Zaporozhets and Akhmetiev, 2013; Zetter et al., 2011).

In this work, we practice the full botanical pollen identification initiated for the Neogene pollen floras in the 1960s (Diniz, 1967; Pons, 1964; Zagwijn, 1960) and intensely developed

since then (Lobreau-Callen and Suc, 1972; Naud and Suc, 1975; Suc, 1971, 1976; Suc and Bessedik, 1981; Jiménez-Moreno and Suc, 2007). Before this evolution, most of the pollen analysts refused to ascribe a botanical name to pollen gains from sediments older than the Pleistocene. The motive adduced was that ante-Quaternary plant species were different from the modern ones. However, significant advances in pollen morphological studies (Erdtman, 1952; Van Campo-Duplan, 1950) resulted in a standardized terminology that documents the large number of characters to be considered for pollen identification (Punt et al., 2007). Detailed knowledge of pollen grains of living plants made possible accurate comparison between fossil pollen and modern pollen from rich collections (often at the comparative microscope and scanning electronic microscope). It was established that identifications were usually possible at the genus level for pre-Quaternary tree pollen grains and family (sometimes genus) level for herbs as synthesized by Suc et al. (2004). Restriction of identifications at the genus level preserves from intra- and inter-specific variability of characters, concealing the palynologist from a no sense specific name. The existence of some modern plant genera since the Early Paleogene has been established for a long time according to plant macroremains (e.g., Schweitzer, 1980; Williams et al., 2003; Eberle and Greenwood, 2012). Now a large majority of palynologists follows this botanical approach for the Neogene sediments because it is the most efficient way for documenting floristic, vegetational and climatic changes based on pollen floras.

The results are shown in synthetic pollen diagrams (Fig. 3), the significance of which has been proven in terms of vegetation changes (Popescu et al., 2010; Suc, 1984; Zagwijn, 1960). Percentages are calculated on the pollen sum excluding *Pinus* that can be over-represented in coastal deltaic sediments (Beaudouin et al., 2005). In the synthetic pollen diagrams, elements are grouped according to a classification of living plants (Nix, 1982) with, from the left to the right: megathermal (tropical) elements (mean annual temperature (MAT)>24°C); mega-

mesothermal (subtropical) elements (20°C<MAT<24°C); *Cathaya*, a conifer living today in tropical-subtropical regions at mid to high elevations but below the *Abies*-*Picea* belt; mesothermal (warm-temperate) elements (14°C<MAT<20°C); meso-microthermal (cool-temperate) elements (12°C<MAT<14°C); microthermal (boreal) elements (MAT<12°C). The right part of the synthetic pollen diagrams is successively occupied by: elements without climatic signification with apart some Cupressaceae (*Juniperus*-*Cupressus*-type), which occupy various biotopes, the pollen of which cannot be identified at the genus level); hygrophilous elements (i.e., water plants); various herbs. The complete pollen floras (with pollen numbers) are shown in Table DR1 and DR2.

3.2. Identification of *Avicennia*.

Several features allow to confidently ascribing pollen grains from the Eocene of Faddeevsky to the genus *Avicennia*. Concerning the apertural system, *Avicennia* from Faddeevsky is represented by equiaxal to slightly longiaxal tricolpate (Fig. DR6: a-c) and tricolporate (Fig. DR6: d-e) pollen grains characterized by long and largely opened colpi (without coastae) that makes the polar triangle very small and the pollen very close to be syncolpate (Fig. DR6: f, h, i). Tricolporate pollen grains show a slightly elongated endoaperture along the polar axis, which does not pass the edges of colpus at the pollen equator. An homobrochate reticulum constitutes the exine sculpture with dense muri (Fig. DR6: a, d, f-i), a little larger than luminae, which are characterized by a polygonal and slightly elongated outline. Thickness of muri somewhat increases toward the poles that reduces the size of luminae (Fig. DR6: b, g). Colpi are bordered by a thin margo where reticulum is smaller. The structure of the semi-tectate ectexine shows dense columellae with large head constituting the tectum overlying a thinner endexine (Fig. DR6: c, e). At scanning electronic microscope, general shape and exine sculpture can be observed in finer detail

showing, in particular, the smooth surface of the tectum somewhat prominent above the columellae (Fig. DR6: g, i). These characters, whatever the pollen is colpate or colporate, are those of the modern *Avicennia* pollen (also supported by a similar size), which unique morphology has been extensively described (Mukherjee and Chanda, 1973) and documented by many photographs at light microscope (Thanikaimoni, 1987). Indeed, the *Avicennia* (colpate or colporate) pollen displays numerous characters that, if considered all together, discard any confusion with pollen grain of other genera. Using both the light and scanning electronic microscopes, the fossil pollen grains have been compared with those of five living species of *Avicennia* (Acanthaceae), selected after meticulous examination of modern pollen photographic atlases. Among them, three species displays pollen morphologies (with a colpate or colporate apertural system) very close to our fossil pollen grains: *A*. *officinalis* L., *A*. *nitida* Jacq., and *A*. *tomentosa* Jacq. (Fig. DR6: k-y), the latter two being synonyms with *A*. *germinans* (L.) L. (see The Plant List website which provides the present-day accepted botanical taxa and synonymies: www.theplantlist.org).

3.3. Ecology of the Eocene Arctic flora and applicability of climate quantification methods based on modern requirements.

Atmospheric carbon dioxide levels and light availability are some of the foremost determinants of higher-plant photosynthesis. As shown in our pollen data, the early-middle Eocene Arctic was covered with extensive forests, composed of mature plants able to produce pollen grains. With a winter of total or near darkness and a summer of continuous, low-angle illumination, these high-latitude forests were characterized by a light regime (photoperiod) without a contemporary counterpart. In these polar forests, trees had to grow under high temperatures and tolerate a highly seasonal insulation regime under very high CO_2 levels (Breecker et al., 2010; West et al., 2015). It could be argued that such conditions may have

301 modified the temperature and water demand of past species (Utescher et al., 2014), thus
302 questioning the applicability of approaches based on modern plant ecology such as that
303 proposed in our study.
304 Experimental studies, however, show that there is no systematic shift of temperature
305 tolerance due to high CO_2, some taxa being more (Wayne et al., 1998) or less (Bertrand et al.,
306 2007; Royer et al., 2002) tolerant to frost stress and some other being unaffected. For
307 instance, experiments with higher atmospheric CO_2 levels increase the frost sensibility of
308 various groups of plants including taxa recorded in Eocene strata of the New Siberian Islands
309 such a 'taxodioid Cupressaceae' or palms (Royer et al., 2002), so that the MTC estimates
310 based on modern plant requirements should be increased by 1.5 to 3°C for times of high CO_2
311 such as during the early Eocene. By contrast, elevated CO_2 diminishes the frost sensibility of
312 one species of *Picea* (Dalen and Johnsen, 2004), a genus also recorded sporadically in the
313 Faddeevsky Island assemblages. Higher CO_2 levels shift the optima for growth of *Avicennia*
314 *germinans* to higher salinities (Reef et al., 2015), but the possible effects on the temperature
315 requirements of this species are unknown. Besides, the evolutionary impact of higher CO_2 on
316 timescales longer than a few years remain poorly understood and needs further investigation
317 (Utescher et al., 2014).
318 Experiments on some Southern Hemisphere tree species have shown that most of the
319 plants were able to tolerate long period of darkness, with a greater tolerance of plants
320 subjected to a 4°C dark treatment than those subjected to a 15°C dark treatment (Read and
321 Francis, 1992). This diminished tolerance to prolonged darkness under warm condition was
322 attributed to the high carbon loss by respiration, as respiration rates increase with increasing
323 temperatures (Lambers et al., 2013). Conversely, continuous light environment can lead to
324 long-term reduction in photosynthetic capacity to avoid hypersaturation of the photosynthesis
325 process (Equiza et al., 2006; Equiza et al., 2005). Experiments have shown that the

326 photosynthetic capacity of some deciduous conifers (*Metasequoia glyptostroboides* H. H. Hu
327 & Cheng, *Larix laricina* (Du Roi) C. Koch and *Taxodium distichum* L. Rich) is significantly
328 reduced by growth under continuous light conditions (24 hours illumination) (Equiza et al.,
329 2006; Equiza et al., 2005). However, it has been suggested that the high atmospheric CO_2
330 levels during the early Eocene reduced carbon respiration during the polar winter and
331 increased photosynthetic carbon gain during the summer, thus improving the survival of high-
332 latitude forests (Axelrod, 1984; Pross et al., 2012).
333 The application of independent proxies may offer a mean of evaluating the validity of our
334 paleoclimate reconstruction method under higher CO_2 and highly seasonal light regimes.
335 Relevant examples are the lower-middle Eocene terrestrial strata of the Canadian Arctic,
336 where physiognomic (West et al., 2015), nearest living relative, faunal (Markwick, 1994) and
337 stable-isotope (Eberle et al., 2010; Jahren and Sternberg, 2003) approaches all yield, within
338 methodological uncertainty, very similar MTC, MAT and MAP estimates (Eberle and
339 Greenwood, 2012). This congruence support the view that the potential biases of pollen-based
340 climate reconstructions linked to high CO_2 and polar photoperiod, although impossible to rule
341 out, should be overall minimal (Utescher et al., 2014).
342
343 **3.4. Vertical distribution of the early-middle Eocene vegetation.**
344 The Faddeevsky Island pollen assemblages suggest coastal forests, inhabited by *Avicennia*,
345 and freshwater swamps (*Glyptostrobus-Taxodium*, and *Nyssa*), with recurrent marine
346 incursions (abundant dinoflagellate cysts in brown mudstone beds at the base of the
347 succession; Fig. 2). Pollen assemblages indicate brackish (Amaranthaceae, *Artemisia*,
348 Caryophyllaceae, *Ephedra*, *Nitraria*, Plumbaginaceae and *Tamarix*: Table DR1) to freshwater
349 marshes (Alismataceae, Menyanthaceae, Onagraceae, *Potamogeton*, *Sparganium*, *Typha* and
350 *Osmunda*) from shoreline to inland (Table DR1), and a shift of forest environments from

evergreen (*Engelhardia*, *Bombax*, *Leea*, *Loropetalum*, Arecaceae, *Distylium*, Rubiaceae, Sapotaceae, *Symplocos*, *Sequoia*-type, etc.) to deciduous associations (*Carya*, *Alnus*, *Acer*, *Eucommia*, *Liquidambar*, *Pterocarya*, *Quercus*) with increasing altitude, both growing in humid climatic and/or edaphic (riparian forests) conditions. *Cathaya*, *Cedrus* and *Tsuga*, *Abies* and *Picea* indicate restricted and relatively distant altitudinal belts, to which *Pinus* may participate.

Similarly, Belkovsky Island pollen assemblages suggest restricted freshwater swamp forests (*Glyptostrobus*-*Taxodium* and *Nyssa*), inland freshwater marshes (Lythraceae, Menyanthaceae, Nymphaeaceae, Onagraceae, *Potamogeton*, Restionaceae, *Ruppia*, *Sparganium*, *Typha*, and *Osmunda*) inhabited by herbs (Cyperaceae) and sporadically invading lowlands (abundant *Azolla* spores in some samples; Table DR2). Forest environments also rapidly shifted from evergreen (*Engelhardia*, Arecaceae, *Sequoia*-type, etc.) to deciduous associations in higher altitude (*Carya*, *Alnus*, *Betula*, *Carpinus*, *Acer*, *Eucommia*, *Liquidambar*, *Myrica*, *Pterocarya*, *Quercus p.p.*, *Salix*, *Ulmus*, *Zelkova*). Large amounts of pollen grains of *Cathaya*, *Tsuga*, and particularly *Abies* and *Picea* indicate developed and nearby altitudinal forests, likely inhabited by *Pinus* (Table DR2).

Climate and vegetation types like those reconstructed for the Eocene of the NSI are nowadays found at much lower latitudes, in the subtropical evergreen broad-leaved forests of Southeastern China (~25 to 30°N and ~110 to 120°E; MAT = 15 to 21°C, MTC = 2 to 12°C, and MAP = 1000 to 2000 mm; Hou, 1983), where *Avicennia marina,* represented by shrubs, is the only mangrove species occurring along the coast (Hou, 1983). The vertical distribution of the vegetation is characterized, from the base to the top of the distant (>1500 km) massifs, by the evergreen broad-leaved forest, mixed evergreen and deciduous (for instance *Betula*, *Acer*) broad-leaved forest, *Cathaya*/*Tsuga* forest, *Picea*/*Abies* forest and high mountain

meadows (Wang, 1961; Hou, 1983). *Abies* develops above 2300 m high and forms pure forests between 3000 and 3200 m.

A complementary vegetation model in line with the proximity of the Verkhoyansk Range suggested by Eocene paleogeographic reconstructions for the NSI (Fig. 1) is that of Taiwan, where the Central Ridge contains over 200 peaks above 3000 m (highest peak at 3952 m) situated near the littoral and steep slopes are common. This mountainous topography results in the formation of distinct altitudinal vegetation zones (foothill, submontane, montane cloud, upper montane and subalpine zones), which correspond to several latitudinal zones from tropical to sub-arctic (Li et al., 2013). The upper-montane coniferous forest is constituted by the *Tsuga–Picea* zone (2500 to 3100 m) and the *Abies* zone (3100 and 3600 m; Su, 1984; Yu et al., 2003). A recent study (Li et al., 2013) found *Abies*/*Tsuga* forests between 2500 and 3400 m, in agreement with those of continental China. The steep slopes near the littoral at Taiwan neither represents a perfect analogue, as *Betula*, *Cathaya* and *Populus* are absent in the high mountain coniferous forests (Lin et al., 2012) and the mangrove includes up to four species (*Avicennia marina*, *Kandelia obovata*, *Lumnitzera racemosa* and *Rhizophora mucronata*; Kao et al., 2004; Li et al., 2013).

In any case, this vertical distribution of modern vegetation strongly suggests that the meso-microtherms and microtherms recorded in the NSI originated from colder nearby massifs of Verkhoyansk and Kolyma, which built-up during the Jurassic-Early Cretaceous (Oxman, 2003; Parfenov et al., 1995) with several peaks still rising today above 2000 m. The subfreezing temperatures and snowfall characterizing winter seasons in the above-mentioned modern regions where *Abies* and *Tsuga* forests grow (Guan et al., 2009; NOAA) suggest that the high-altitude regions of Arctic Siberia were certainly characterized by much cooler MATs and MTC than those deduced from our climatic reconstruction of low-altitude vegetation.

400 **4. Organic matter source and preservation.**

401 The unusually wide range of Tmax (between 353 and 437 °C) and HI (up to 450 mg HC/g
402 TOC) values recorded in the Faddeevsky Island section is partly attributable to the presence
403 of abundant amber particles (Fig. DR3) which yield hydrocarbons at very low temperature
404 and possess a very HI-value (>1000 mg HC/g TOC) in the pure amber aliquot (Table DR3).
405 The sum of amber + *Botryococcus* + Amorphous Organic Matter (AOM) particles determined
406 in the palynofacies assemblages show a good positive correlation with HI (R^2=0.59),
407 indicating that an additional contribution to the hydrogen-rich fraction comes from
408 *Botryococcus* and AOM, which can both contain elevated amount of lipids (Metzger and
409 Largeau, 2005; Tyson, 1995). We attribute the very high Tmax (609°C) value of the pre-
410 PETM sample at Faddeevsky to the elevated amounts of fusinite (charcoal), which represents
411 24% of the particles in the palynofacies residue of the same sample (Fig. DR3). The
412 anomalously high abundance in this sample of monolete and trilete Pteridophyte spores
413 contributing to the lower vegetation layer (Table DR1), which are mostly transported by water
414 run-off (Suc, 1976), indicate more open conditions that may have resulted from post-fire
415 erosion. The occurrence of lower but non-negligible amounts of opaque phytoclast debris
416 (palynomaceral 4) in both successions (Fig. DR3) indicates less frequent forest fires near the
417 study area throughout the study interval. Such forest fires, in relation with precipitation
418 regimes, may have been critical factors for the growth of Arctic deciduous relative to
419 evergreen biomes in greenhouse climates (Brentnall et al., 2005).

420 Samples without amber plot in the area of Type II, III and IV kerogen in the modified van
421 Krevelen diagram (Fig. DR7), indicating the dominance of terrestrial higher plants debris and
422 highly oxidized organic matter, and a subordinate but substantial contribution of a lipid-rich
423 fraction of terrestrial origin. The elevated proportions of higher-plant derived particles in
424 palynofacies (Palynomaceral 1+2, Palynomaceral 3 and Palynomaceral 4) also reveal a

425 generally dominant terrestrial component. The amber particles have a markedly higher $\delta^{13}C$
426 composition (–22.68‰; Table DR3) than bulk organic carbon and wood particles. The
427 organic carbon isotope composition of bulk sediment samples ($\delta^{13}C_{TOC}$), however, correlates
428 poorly with C/N ratios, Rock-Eval parameters and the abundance of different palynological
429 particles (Fig. DR3; Table DR4). This suggests that the recorded fluctuations likely reflect
430 primary change in environmental conditions rather than changing amounts of particles with
431 distinct isotope compositions.
432 The low Tmax values (from 383 °C to 407°C) recorded at Belkovsky Island indicate an
433 immature stage of the organic matter with respect to the oil generation. The organic matter is
434 distributed between Type III and Type IV in a modified van Krevelen diagram (Fig. DR7) and
435 thus corresponds to terrestrial higher plants debris and highly oxidized organic matter, in
436 accordance with palynofacies results that generally show dominant Palynomaceral 1+2,
437 Palynomaceral 3 and Palynomaceral 4 (Fig. DR3). The $\delta^{13}C_{TOC}$ values show a good linear
438 inverse correlation with C/N ratios (R^2=0.71), C/S ratios (R^2=0.51) and the amount of
439 Amorphous Organic Matter (R^2=0.48), a good inverse logarithmic correlation with TOC
440 values (R^2=0.79) and a moderate positive correlation with OI values (R^2=0.36), the amount of
441 pollen and spores (R^2=0.37) and opaque phytoclast (Palynomaceral 4) particles deduced from
442 palynofacies (R^2=0.37). These correlations (Table DR4) strongly suggest that the recorded
443 changes in $\delta^{13}C_{TOC}$ at Belkovsky Island are mainly attributable to a mixing of different
444 components with distinct $\delta^{13}C_{TOC}$ values, with the low $\delta^{13}C_{TOC}$ values being characteristic of
445 less oxidized organic matter, as reflected by lower OI, higher TOC, higher C/N ratios and
446 lower contents of strongly oxidized terrestrial phytoclasts (Palynomaceral 4). The higher
447 abundance of structured cuticle and epidermis particles (Palynomaceral 3) (less oxidized)
448 particles between 0.8 and 1.8 m (Fig. DR3) also indicates more reducing conditions in the
449 interval recording lower $\delta^{13}C_{TOC}$ values. These data are in line with the increase in $\delta^{13}C_{TOC}$

values recorded in modern plants with increasing oxidation (Gröcke, 1998; van Bergen and Poole, 2002). Changes in $\delta^{13}C_{TOC}$ values at Belkovsky Island are thus essentially attributable to differential oxidation and cannot be used to correlate the section with other marine or terrestrial records.

5. Oxygenation and sulfate availability.

Our mineralogical analyses show that sulfur-rich minerals are represented by pyrite and jarosite in the two sections. Jarosite contents are much higher and, unlike those of pyrite, parallel the TS contents (Fig. DR3). Jarosite in coastal plain sediment is considered to result from the oxidation of pyrite under well-oxygenated conditions, either in soils shortly after deposition or in subsurface due to recent exposure (Kraus, 1998). In any case, substantial amounts of both minerals in the investigated successions points to deposition under reduced conditions with high organic matter and sulfide availability, implying recurrent intermixing of marine or tidal sulfate-rich waters with pore fluids of the coastal plain sediments (Ufnar et al., 2001).

The Faddeevsky succession contains several siderite-rich levels, which occur as nodular beds along unit IIf and IIIf (Fig. DR2) and are illustrated by the high siderite contents of the collected samples in our DRX data (Fig. DR3). Siderite is considered as reflecting high organic matter and iron supply in reduced conditions with limited sulfate availability in pore fluids (Ufnar et al., 2001). Such a sulfate limitation is supported by the mutual exclusion of pyrite and siderite in the same samples at Faddeevsky (Fig. DR3). The occurrence of siderite at Faddeevsky is also climatically significant, as its presence in Eocene and Cretaceous paleosoils of Arctic Canada and Alaska has been suggested to reflect saturated soil acidity and methane production in organic-rich wetlands (Ludvigson et al., 1998).

Supplementary references

Axelrod, D. I., 1984, An interpretation of Cretaceous and tertiary biota in polar regions: Palaeogeography, Palaeoclimatology, Palaeoecology, v. 45, no. 2, p. 105-147.

Barke, J., van der Burgh, J., van Konijnenburg-van Cittert, J. H. A., Collinson, M. E., Pearce, M. A., Bujak, J., Heilmann-Clausen, C., Speelman, E. N., van Kempen, M. M. L., Reichart, G.-J., Lotter, A. F., and Brinkhuis, H., 2012, Coeval Eocene blooms of the freshwater fern *Azolla* in and around Arctic and Nordic seas: Palaeogeography, Palaeoclimatology, Palaeoecology, v. 337–338, p. 108-119.

Batten, D. J., 1981, The *Normapolles* Group and Province Stratigraphic, palaeogeographic and evolutionary significance of late cretaceous and early tertiary normapolles pollen: Review of Palaeobotany and Palynology, v. 35, no. 2, p. 125-137.

Beaudouin, C., Suc, J.-P., Cambon, G., Touzani, A., Giresse, P., Pont, D., Aloïsi, J.-C., Marsset, T., Cochonat, P., Duzer, D., and Ferrier, J., 2005, Present-day rhythmic deposition in the Grand Rhône prodelta (NW Mediterranean) according to high-resolution pollen analyses: Journal of Coastal Research, v. 21, p. 292–306.

Behar, F., Beaumont, V., and De B. Penteado, H. L., 2001, Technologie Rock-Eval 6 : performances et développements: Oil & Gas Science and Technology - Rev. IFP, v. 56, no. 2, p. 111-134.

Bertrand, A., Prévost, D., Bigras, F. J., and Castonguay, Y., 2007, Elevated atmospheric CO_2 and strain of Rhizobium alter freezing tolerance and cold-induced molecular changes in Alfalfa (*Medicago sativa*): Annals of Botany, v. 99, no. 2, p. 275-284.

Bessedik, M., 1984, The early Aquitanian and upper Langhian-Lower Serravallian environments in the Northwestern Mediterranean region: Paléobiologie continentale, v. 14, no. 2, p. 153-179.

Breecker, D. O., Sharp, Z. D., and McFadden, L. D., 2010, Atmospheric CO_2 concentrations during ancient greenhouse climates were similar to those predicted for A.D. 2100: Proceedings of the National Academy of Sciences, v. 107, no. 2, p. 576-580.

Brentnall, S. J., Beerling, D. J., Osborne, C. P., Harland, M., Francis, J. E., Valdes, P. J., and Wittig, V. E., 2005, Climatic and ecological determinants of leaf lifespan in polar forests of the high CO_2 Cretaceous 'greenhouse' world: Global Change Biology, v. 11, no. 12, p. 2177-2195.

Brinkhuis, H., Schouten, S., Collinson, M. E., Sluijs, A., Damste, J. S. S., Dickens, G. R., Huber, M., Cronin, T. M., Onodera, J., Takahashi, K., Bujak, J. P., Stein, R., van der Burgh, J., Eldrett, J. S., Harding, I. C., Lotter, A. F., Sangiorgi, F., Cittert, H. V. V., de Leeuw, J. W., Matthiessen, J., Backman, J., and Moran, K., 2006, Episodic fresh surface waters in the Eocene Arctic Ocean: Nature, v. 441, no. 7093, p. 606-609.

Brown, G., Brindley, G. W., and Brown, G., 1980, Crystal structures of clay minerals and their X-ray identification: Mineralogical Society, London, p. 361-410.

Bujak, J. P., and Brinkhuis, H., 1998, Global warming and dinocyst changes across the Paleocene/Eocene Epoch boundary, *in* Aubry, M.-P., Lucas, S. G., and Berggren, W. A., eds., Late Paleocene-early Eocene climatic and biotic events in the marine and terrestrial records: New York, Columbia University Press, p. 277-295.

Cogné, J.-P., Besse, J., Chen, Y., and Hankard, F., 2013, A new Late Cretaceous to Present APWP for Asia and its implications for paleomagnetic shallow inclinations in Central Asia and Cenozoic Eurasian plate deformation: Geophysical Journal International, v. 192, no. 3, p. 1000-1024.

Cour, P., 1974, Nouvelles techniques de detection des flux et des retombees polliniques: Etude de la sedimentation des pollens et des s pores a la surface du sol: Pollen et spores.

524 Crouch, E. M., Brinkhuis, H., Visscher, H., Adatte, T., and Bolle, M.-P., 2003, Late
525 Paleocene-early Eocene dinoflagellate cyst records from the Tethys: Further
526 observations on the global distribution of Apectodinium: Geological Society of
527 America Special Papers, v. 369, p. 113-131.
528 Crouch, E. M., Heilmann-Clausen, C., Brinkhuis, H., Morgans, H. E. G., Rogers, K. M.,
529 Egger, H., and Schmitz, B., 2001, Global dinoflagellate event associated with the late
530 Paleocene thermal maximum: Geology, v. 29, no. 4, p. 315-318.
531 Dalen, L., and Johnsen, Ø., 2004, CO_2 enrichment, nitrogen fertilization and development of
532 freezing tolerance in Norway spruce: Trees, v. 18, no. 1, p. 10-18.
533 Diniz, F., 1967, Une flore tertiaire de caractère méditerranéen au Portugal: Review of
534 Palaeobotany and Palynology, v. 5, p. 262–268.
535 Eberle, J. J., Fricke, H. C., Humphrey, J. D., Hackett, L., Newbrey, M. G., and Hutchison, J.
536 H., 2010, Seasonal variability in Arctic temperatures during early Eocene time: Earth
537 and Planetary Science Letters, v. 296, no. 3–4, p. 481-486.
538 Eberle, J. J., and Greenwood, D. R., 2012, Life at the top of the greenhouse Eocene world– A
539 review of the Eocene flora and vertebrate fauna from Canada's High Arctic:
540 Geological Society of America Bulletin, v. 124, no. 1-2, p. 3-23.
541 Eldrett, J. S., Greenwood, D. R., Harding, I. C., and Huber, M., 2009, Increased seasonality
542 through the Eocene to Oligocene transition in northern high latitudes: Nature, v. 459,
543 p. 969–973.
544 Eldrett, J. S., Greenwood, D. R., Polling, M., Brinkhuis, H. and Sluijs, A., 2014,A seasonality
545 trigger for carbon injection at the Paleocene–Eocene Thermal Maximum: Climate of
546 the Past, v. 10, p. 759–769.
547 Equiza, M. A., Day, M. E., and Jagels, R., 2006, Physiological responses of three deciduous
548 conifers (*Metasequoia glyptostroboides*, *Taxodium distichum*, *Larix laricina*) to a
549 continuous-light environment: adaptative implications for the early-Tertiary polar
550 summer: Tree physiology, v. 26, p. 353-364.
551 Equiza, M. A., Day, M. E., Jagels, R., and Li, X., 2005, Photosynthetic downregulation in the
552 conifer *Metasequoia glyptostroboides* growing under continuous light: the
553 significance of carbohydrate sinks and paleoecophysiological implications: Canadian
554 Journal of Botany, v. 84, p. 1453-1461.
555 Erdtman, G., 1952, Pollen morphology and plant taxonomy., Stockholm, Almqvist & Wiksell.
556 Fauquette, S., Guiot, J., and Suc, J.-P., 1998, A method for climatic reconstruction of the
557 Mediterranean Pliocene using pollen data: Palaeogeography, Palaeoclimatology,
558 Palaeoecology, v. 144, p. 183–201.
559 Franke, D., and Hinz, K., 2009, Geology of the shelves surrounding the New Siberian Islands,
560 Russian Arctic., *in* D. B. Stone, K. F., P. W. Layer, E. L. Miller, A. V. Prokopiev, J.
561 Toro, ed., Geology, geophysics and tectonics of Northeastern Russia: a tribute to
562 Leonid Parfenov, Volume 4, Stephan Mueller Spec. Publ. Ser., p. 35-44.
563 Frederiksen, N. O., Edwards, L. E., Ager, T. A., and Sheehan, T. P., 2002, Palynology of
564 Eocene strata in the Sagavanirktok and Canning formations on the north slope of
565 Alaska: Palynology, v. 26, p. 59–93.
566 Friis, E. M., Pedersen, K. R., and Schönenberger, J., 2006, *Normapolles* plants: a prominent
567 component of the Cretaceous rosid diversification: Plant Systematics and Evolution, v.
568 260, no. 2-4, p. 107-140.
569 Gaina, C., Roest, W. R., and Muller, R. D., 2002, Late Cretaceous-Cenozoic deformation of
570 northeast Asia: Earth and Planetary Science Letters, v. 197, no. 3-4, p. 273-286.
571 Gröcke, D. R., 1998, Carbon-isotope analyses of fossil plants as a chemostratigraphic and
572 palaeoenvironmental tool: Lethaia, v. 31, no. 1, p. 1-13.

Guan, B. T., Hsu, H.-W., Wey, T.-H., and Tsao, L.-S., 2009, Modeling monthly mean temperatures for the mountain regions of Taiwan by generalized additive models: Agricultural and Forest Meteorology, v. 149, no. 2, p. 281-290.

Harrington, G. J., Eberle, J., Le-Page, B. A., Dawson, M., and Hutchison, J. H., 2012, Arctic plant diversity in the Early Eocene greenhouse: Proceedings of the Royal Society, Series B, v. 279, p. 1515–1521.

Holtzapffel, T., 1985, Les minéraux argileux préparation, analyse diffractométrique et détermination, Villeneuve d'Ascq, Société géologique du Nord, Publication 12, 1 vol. (136 p.) p.:

Hou, H.-Y., 1983, Vegetation of China with reference to its geographical distribution: Annals of Missouri Botanical Garden, v. 70, p. 509-548.

Iakovleva, A. I., 2016, Did the PETM trigger the first important radiation of wetzelielloideans? Evidence from France and northern Kazakhstan: Palynology, p. 1-28.

Iakovleva, A. I., and Kulkova, I. A., 2003, Paleocene–Eocene dinoflagellate zonation of Western Siberia: Review of Palaeobotany and Palynology, v. 123, no. 3–4, p. 185-197.

Jahren, A. H., and Sternberg, L. S. L., 2003, Humidity estimate for the middle Eocene Arctic rain forest: Geology, v. 31, p. 463-466.

Jiménez-Moreno, G., and Suc, J.-P., 2007. Middle Miocene latitudinal climatic gradient in Western Europe: Evidence from pollen records. Palaeogeography, Palaeoclimatology, Palaeoecology, v. 253, 224–241.

Kalkreuth, W. D., McIntyre, D. J., and Richardson, R. J. H., 1993, The geology, petrography and palynology of Tertiary coals from the Eureka Sound Group at Strathcona Fiord and Bache Peninsula, Ellesmere Island, Arctic Canada: International Journal of Coal Geology, v. 24, p. 75–111.

Kalkreuth, W. D., Riediger, C. L., McIntyre, D. J., Richardson, R. J. H., Fowler, M. G., and Marchioni, D., 1996, Petrological, palynological and geochemical characteristics of Eureka Sound Group coals (Stenkul Fiord, southern Ellesmere island, Arctic Canada): International Journal of Coal Geology, v. 30, p. 151–182.

Kao, W.-Y., Shih, C.-N., and Tsai, T.-T., 2004, Sensitivity to chilling temperatures and distribution differ in the mangrove species *Kandelia candel* and *Avicennia marina*: Tree Physiology, v. 24, no. 7, p. 859-864.

Kirtland Turner, S., Sexton, P. F., Charles, C. D., and Norris, R. D., 2014, Persistence of carbon release events through the peak of early Eocene global warmth: Nature Geoscience, v. 7, no. 10, p. 748-751.

Kos'ko, M. K., and Trufanov, G. V., 2002, Middle Cretaceous to Eopleistocene Sequences on the New Siberian Islands: an approach to interpret offshore seismic: Marine and Petroleum Geology, v. 19, no. 7, p. 901-919.

Kos'ko, M., and Korago, E., 2009, Review of geology of the New Siberian Islands between the Laptev and the East Siberian Seas, North East Russia, *in* Stone, D. B., Fujita, K., Layer, P. W., Miller, E. L., Prokopiev, A. V., and Toro, J., eds., Stephan Mueller Special Publication Series - Geology, geophysics and tectonics of Northeastern Russia: a tribute to Leonid Parfenov, p. 45-64.

Kraus, M. J., 1998, Development of potential acid sulfate paleosols in Paleocene floodplains, Bighorn Basin, Wyoming, USA: Palaeogeography, Palaeoclimatology, Palaeoecology, v. 144, no. 1–2, p. 203-224.

Kuzmichev, A. B., Aleksandrova, G. N., Herman, A. B., Danukalova, M. K., and Simakova, A. N., 2013, Paleogene-Neogene sediments of Bel'kov Island (New Siberian Islands):

Characteristics of sedimentary cover in the eastern Laptev shelf: Stratigraphy and Geological Correlation, v. 21, no. 4, p. 421-444.
Lambers, H., Chapin, F. S., and Pons, T. L., 2013, Plant Physiological Ecology, Springer Science & Business Media.
Li, C. F., Chytry, M., Zeleny, D., Chen, M. Y., Chen, T. Y., Chiou, C. R., Hsia, Y. J., Liu, H. Y., Yang, S. Z., Yeh, C. L., Wang, J. C., Yu, C. F., Lai, Y. J., Chao, W. C., and Hsieh, C. F., 2013, Classification of Taiwan forest vegetation: Applied Vegetation Science, v. 16, p. 698-719.
Lin, C. T., Li, C. F., Zeleny, D., Chytry, M., Nakamura, Y., Chen, T. Y., Hsia, Y. J., Hsieh, C. F., Liu, H. Y., Wang, J. C., Yang, S. Z., Yeh, C. L., and Chiou, C. R., 2012, Classification of the high-mountain coniferous forests in Taiwan: Folia Geobotanica, v. 47, p. 373-401.
Liu, Y.-S., and Basinger, J. F., 2000, Fossil *Cathaya* (Pinaceae) pollen from the Canadian high Arctic: International Journal of Plant Science, v. 161, no. 5, p. 829–847.
Lobreau-Callen, D., and Suc, J.-P., 1972, Présence de pollens de *Microtropis fallax* (Celastraceae) dans le Pléistocène inférieur de Celleneuve (Hérault): Comptes-Rendus de l'Académie des Sciences de Paris, v. 275, no. ser. D, p. 1351–1354.
Ludvigson, G. A., González, L. A., Metzger, R. A., Witzke, B. J., Brenner, R. L., Murillo, A. P., and White, T. S., 1998, Meteoric sphaerosiderite lines and their use for paleohydrology and paleoclimatology: Geology, v. 26, no. 11, p. 1039-1042.
Markwick, P. J., 1994, "Equability," continentality, and Tertiary "climate": The crocodilian perspective: Geology, v. 22, no. 7, p. 613-616.
McCabe, P. J., 1990, Coal Geology: Geotimes, v. 35, no. 2, p. 20-20.
Metzger, P., and Largeau, C., 2005, *Botryococcus braunii:* a rich source for hydrocarbons and related ether lipids: Applied Microbiology and Biotechnology, v. 66, no. 5, p. 486-496.
Moore, D. M., and Reynolds, R. C., 1989, X-ray Diffraction and the Identification and Analysis of Clay Minerals, Oxford university press Oxford.
Moran, K., Backman, J., Brinkhuis, H., Clemens, S. C., Cronin, T., Dickens, G. R., Eynaud, F., Gattacceca, J., Jakobsson, M., Jordan, R. W., Kaminski, M., King, J., Koc, N., Krylov, A., Martinez, N., Matthiessen, J., McInroy, D., Moore, T. C., Onodera, J., O'Regan, M., Pälike, H., Rea, B., Rio, D., Sakamoto, T., Smith, D. C., Stein, R., St John, K., Suto, I., Suzuki, N., Takahashi, K., Watanabe, M., Yamamoto, M., Farrell, J., Frank, M., Kubik, P., Jokat, W., and Kristoffersen, Y., 2006, The Cenozoic palaeoenvironment of the Arctic Ocean: Nature, v. 441, no. 7093, p. 601-605.
Mukherjee, J., and Chanda, S., 1973, Biosynthesis of Avicennia L. in relation to taxonomy: Geophytology, v. 3, p. 85-88.
Naud, G., and Suc, J.-P., 1975, Contribution à l'étude paléofloristique des Coirons (Ardèche): premières analyses polliniques dans les alluvions sous-basaltiques et interbasaltiques de Mirabel (Miocène supérieur): Bulletin de la Société géologique de France, v. 17, no. 5, ser. 7, p. 820–827.
Nix, H., 1982, Environmental determinants of biogeography and evolution in Terra Australis, *in* Barker, W. R., and Greenslade, P. J. M., eds., Evolution of the Flora and fauna of Arid Australia: Frewville, Peacock Publishing, p. 47–66.
NOAA, http://www.ncdc.noaa.gov/.
Oxman, V. S., 2003, Tectonic evolution of the Mesozoic Verkhoyansk–Kolyma belt (NE Asia): Tectonophysics, v. 365, no. 1–4, p. 45-76.
Parfenov, L. M., Prokopiev, A. V., and Gaiduk, V. V., 1995, Cretaceous frontal thrusts of the Verkhoyansk fold belt, eastern Siberia: Tectonics, v. 14, no. 2, p. 342-358.

Pons, A., 1964, Contribution palynologique à l'étude de la flore et de la végétation pliocènes de la région rhodanienne: Annales des Sciences Naturelles, Botanique, v. 5, no. ser. 12, p. 499–722.
Popescu, S.-M., Biltekin, D., Winter, H., Suc, J.-P., Melinte-Dobrinescu, M. C., Klotz, S., Combourieu-Nebout, N., Rabineau, M., Clauzon, G., and Deaconu, F., 2010, Pliocene and Lower Pleistocene vegetation and climate changes at the European scale: Long pollen records and climatostratigraphy: Quaternary International, v. 219, p. 152–167.
Pross, J., Contreras, L., Bijl, P. K., Greenwood, D. R., Bohaty, S. M., Schouten, S., Bendle, J. A., Rohl, U., Tauxe, L., Raine, J. I., Huck, C. E., van de Flierdt, T., Jamieson, S. S. R., Stickley, C. E., van de Schootbrugge, B., Escutia, C., Brinkhuis, H., and Scientists, a. I. O. D. P. E., 2012, Persistent near-tropical warmth on the Antarctic continent during the early Eocene epoch: Nature, v. 488, no. 7409, p. 73-77.
Punt, W., Hoen, P. P., Blackmore, S., Nilsson, S., and Le Thomas, A., 2007, Glossary of pollen and spore terminology: Review of Palaeobotany and Palynology, v. 143, p. 1–81.
Read, J., and Francis, J., 1992, Responses of some Southern Hemisphere tree species to a prolonged dark period and their implications for high-latitude Cretaceous and Tertiary floras: Palaeogeography, Palaeoclimatology, Palaeoecology, v. 99, no. 3, p. 271-290.
Reef, R., Winter, K., Morales, J., Adame, M. F., Reef, D. L., and Lovelock, C. E., 2015, The effect of atmospheric carbon dioxide concentrations on the performance of the mangrove *Avicennia germinans* over a range of salinities: Physiol Plant, v. 154, no. 3, p. 358-368.
Ridgway, K. D., Sweet, A. R., and Cameron, A. R., 1995, Climatically induced floristic changes across the Eocene–Oligocene transition in the northern high latitudes, Yukon Territory, Canada: Geological Society of America Bulletin, v. 107, no. 6, p. 676–696.
Royer, D. L., Osborne, C. P., and Beerling, D. J., 2002, High CO_2 increases the freezing sensitivity of plants: Implications for paleoclimatic reconstructions from fossil floras: Geology, v. 30, no. 11, p. 963-966.
Schweitzer, H.-J., 1980, Environment and climate in the early tertiary of spitsbergen: Palaeogeography, Palaeoclimatology, Palaeoecology, v. 30, p. 297-311.
Sluijs, A., Brinkhuis, H., Crouch, E. M., John, C. M., Handley, L., Munsterman, D., Bohaty, S. M., Zachos, J. C., Reichart, G. J., Schouten, S., Pancost, R. D., Damste, J. S. S., Welters, N. L. D., Lotter, A. F., and Dickens, G. R., 2008, Eustatic variations during the Paleocene-Eocene greenhouse world: Paleoceanography, v. 23, no. 4.
Sluijs, A., Schouten, S., Pagani, M., Woltering, M., Brinkhuis, H., Damste, J. S. S., Dickens, G. R., Huber, M., Reichart, G. J., Stein, R., Matthiessen, J., Lourens, L. J., Pedentchouk, N., Backman, J., and Moran, K., 2006, Subtropical arctic ocean temperatures during the Palaeocene/Eocene thermal maximum: Nature, v. 441, no. 7093, p. 610-613.
Su, H. J., 1984, Studies on the climate and vegetation types of the natural forests in Taiwan: 1. Analysis in variation of climate factors: Quarterly Journal of Chinese Forestry, v. 17, p. 1–14.
Suc, J.-P., 1971, Présence d'un faciès fluvio-marin dans les marnes à micro-mammifères de Celleneuve (Hérault): Bulletin de l'Association française d'étude du Quaternaire, v. 4, p. 251–258.
-, 1976, Quelques taxons-guides dans l'étude paléoclimatique du Pliocène et du Pléistocène inférieur du Languedoc (France): Revue de Micropaléontologie v. 18, no. 4, p. 246–255.
-, 1984, Origin and evolution of the Mediterranean vegetation and climate in Europe: Nature, v. 307, no. 5950, p. 429–432.

Suc, J.-P., and Bessedik, M., 1981, A methodology for Neogene palynostratigraphy: International Symposium on Concepts and Methods in Paleontology, p. 205–208.
Suc, J.-P., Fauquette, S., and Popescu, S.-M., L'investigation palynologique du Cénozoïque passe par les herbiers. Bulletin de la Société Botanique de France, *in* Proceedings "Les herbiers: un outil d'avenir. Tradition et modernité", Villeurbanne, 2004, Association française pour la Conservation des Espèces Végétales, p. 67–87.
Thanikaimoni, G., 1987, Mangrove palynology, Institut Français de Pondichéry,, Travaux de la Section Scientifique et technique.
Tyson, R. V., 1995, Sedimentary organic matter: organic facies and palynofacies, Chapman & Hall.
Ufnar, D. F., González, L. A., Ludvigson, G. A., Brenner, R. L., and Witzke, B. J., 2001, Stratigraphic Implications of Meteoric Sphaerosiderite δ18O Values in Paleosols of the Cretaceous (Albian) Boulder Creek Formation, NE British Columbia Foothills, Canada: Journal of Sedimentary Research, v. 71, no. 6, p. 1017-1028.
Utescher, T., Bruch, A. A., Erdei, B., François, L., Ivanov, D., Jacques, F. M. B., Kern, A. K., Liu, Y. S., Mosbrugger, V., and Spicer, R. A., 2014, The Coexistence Approach—Theoretical background and practical considerations of using plant fossils for climate quantification: Palaeogeography, Palaeoclimatology, Palaeoecology, v. 410, p. 58-73.
van Bergen, P. F., and Poole, I., 2002, Stable carbon isotopes of wood: a clue to palaeoclimate?: Palaeogeography, Palaeoclimatology, Palaeoecology, v. 182, no. 1-2, p. 31-45.
Van Campo-Duplan, M., 1950, Recherches sur la phylogénie des Abiétinées d'après leurs grains de pollen: Travaux du Laboratoire forestier de Toulouse, v. 2, no. sect. 1, p. 9–182.
Vandenberghe, N., Hilgen, F. J., and Speijer, R. P., 2012, The Paleogene Period: The Geologic Time Scale, v. 2012, p. 855-921.
van Hinsbergen, D. J. J., de Groot, L. V., van Schaik, S. J., Spakman, W., Bijl, P. K., Sluijs, A., Langereis, C. G., and Brinkhuis, H., 2015, A Paleolatitude Calculator for Paleoclimate Studies: PLOS ONE, v. 10, no. 6, p. e0126946.
Wang, C.-W, 1961. The forests of China with a survey of grassland and desert vegetation. Maria Moors Cabot Foundation, 5, Harvard University, Cambridge, Massachusetts, 313 p.
Wayne, P. M., Reekie, E. G., and Bazzaz, F. A., 1998, Elevated CO_2 ameliorates birch response to high temperature and frost stress: implications for modeling climate-induced geographic range shifts: Oecologia, v. 114, no. 3, p. 335-342.
West, C. K., Greenwood, D. R., and Basinger, J. F., 2015, Was the Arctic Eocene 'rainforest' monsoonal? Estimates of seasonal precipitation from early Eocene megafloras from Ellesmere Island, Nunavut: Earth and Planetary Science Letters, v. 427, p. 18-30.
Whitaker, M. F., 1984, The usage of palynostratigraphy and palynofacies in definition of Troll Field geology, 6th Offshore Northern Seas Conference and Exhibition, Stavanger 1984, Volume Paper G6, Norsk Petroleumsforening, p. 44.
Williams, C. J., Johnson, A. H., LePage, B. A., Vann, D. R., and Sweda, T., 2003, Reconstruction of Tertiary Metasequoia forests. II. Structure, biomass, and productivity of Eocene floodplain forests in the Canadian Arctic: Paleobiology, v. 29, no. 2, p. 271-292.
Williams, G. L., Damassa, S. P., Fensome, R. A., and Guerstein, G. R., 2015, Wetzeliella and Its Allies — The 'Hole' Story: A Taxonomic Revision of the Paleogene Dinoflagellate Subfamily Wetzelielloideae: Palynology, v. 39, no. 3, p. 289-344.
Yu, G., Liew, P., Xue, B., and Li, Z., 2003, Surface pollen and vegetation reconstruction from central and northern Taiwan: Chinese Science Bulletin, v. 48, no. 3, p. 291-295.

771 Zagwijn, W. H., 1960, Aspects of the Pliocene and early Pleistocene vegetation in The
772 Netherlands: Mededelingen van de Geologische Stichting, v. 3, no. 5, ser. C, p. 1–78.
773 Zaporozhets, N. I., and Akhmetiev, M. A., 2013, The Middle and Upper Eocene sections of
774 the omsk Trough, West Siberian Platform: Palynological, stratigraphic, hydrologic,
775 and climatic aspects: Stratigrafiya, Geologicheskaya Korrelyatsita, v. 21, no. 1, p.
776 102–126.
777 Zetter, R., Farabee, M. J., Pigg, K. B., Manchester, S. R., DeVore, M. L., and Nowal, M. D.,
778 2011, Palynoflora of the late Paleocene silicified shale at Almont, North Dakota,
779 USA: Palynology, v. 35, no. 2, p. 179–211.

780
781

Table DR1. Pollen flora of the Faddeevsky Island section. Taxa are organized with respect to their ecological significance. Identification nomenclature: cf., used to reveal which living taxon (species, genus) has the nearest pollen morphology to the fossil pollen within a taxonomic entity (genus, family); -type, used to indicate a pollen-type within a taxonomic entity (genus, family) without a robust significance as identification. Symbols: *, halophyte; X, present.

Sample number	GS114	GS115	GS116	GS117	GS118	GS119	GS120	GS121	GS122	GS123	GS124	GS125	GS126	GS127	GS128	GS129	GS130	GS131	GS132	GS133	GS134	GS135	GS136	GS137
Height (m)	1.05	1.80	1.95	2.05	2.45	2.75	3.20	3.85	4.15	4.55	5.00	5.50	6.10	6.50	7.00	7.60	8.30	18.45	23.60	29.50	30.80	31.75	32.70	35.00
MEGATHERMIC TREES (OR LIANAS)																								
Altingia (Altingiaceae)															1									
*Avicennia** (Acanthaceae)						1					4			3			3	2	1		1		2	1
Bombax (Malvaceae)															1									
Buxus bahamensis-type (Buxaceae)																	1							
Citrus (Rutaceae)							1																	
Mimosoideae (Leguminosae)																						1		
Passifloraceae													1											
Morinda-type (Rubiaceae)																	1							
MEGA-MESOTHERMIC TREES (OR LIANAS)																								
cf. *Araucaria* (Araucariaceae)	1																							
Cathaya (Pinaceae)	1			5	2	3	15			1	1				1		1		1	5	2		1	1
Glyptostrobus-Taxodium (Cupressaceae)		35	35	50	22	32	1	11	37	34	9	39	32	5	12	14	17	11	12	40	3	8	12	16
Sequoia-type (Cupressaceae)	1	17	10	3	37	17	2			13	10	28	13	8	6	1	3	7	10	26	4	2	5	12
Arecaceae		2									1						3							
Celastraceae			1	1								1		1		1	1		1		1		1	
Cyrillaceae-Clethraceae															5									
Distylium (Hamamelidaceae)		1											1				1					1		
Engelhardia (Juglandaceae)	1	5	5	10	1	4	1	2	8	6	10	6	4	8	2	12	2	7	5	18	38	60	3	2
Fothergilla (Hamamelidaceae)																			1					
Hamamelis (Hamamelidaceae)															1									
Icacinaceae														1		1								
Ilex floribunda-type (Aquifoliaceae)																			1					
Leea (Vitaceae)														2		1		1					1	
Loropetalum (Hamamelidaceae)		1							1				1				1							
Matudaea (Hamamelidaceae)									1															
Menispermaceae				1						1		1												
Microtropis (Celastraceae)																	1							
Moraceae																		2						
Nyssa (Cornaceae)				1				4	3		2	1		3		2	2				2		1	
Nyssa cf. *sinensis* (Cornaceae)		3				2				2	2	1	1	19	1	2		2	2	1				1
Rhodoleia (Hamamelidaceae)										1		1												
Mussaenda-type (Rubiaceae)															1									
Uncaria- type (Rubiaceae)		1											2					1						
Sapotaceae						1							1		1			1	1					
Symplocos (Symplocaceae)							2						1											
MESOTHERMIC TREES (OR LIANAS)																								
Acer (Sapindaceae)		1							1			3		1	3		1	2	2	2	2			3
Aesculus (Sapindaceae)											1		1											
Alnus (Betulaceae)	3	3	20	11	15	2	13	55		3	18	4	8	2	6	9	4	8	2	3	17	1	3	27
Araliaceae																								2
Betula-type (Betulaceae)	3						1									1	2					1		
Betula (Betulaceae)	14						3		1								1			1				
Buxus sempervirens-type (Buxaceae)												1					1	1						1
Carpinus (Betulaceae)	2						1	1	3		1						3		3		2		6	
Carya (Juglandaceae)		4	6	6	1	8	5	1	11	9	6		7	12	7	9	12	12	12	3	3	2	18	15
Castanea-Castanopsis (Fagaceae)			4			7	1	2	2	1	8		14	9	2	1	1	5	2		7	9	2	2
Celtis (Cannabaceae)						1	1										2				1		1	
Decodon (Lythraceae)											1		2		1									
Ericaceae	7	3	1	3		3	7	3	2	5	11	2	2	7	1		2	1	3	9	7	2	2	1
Eucommia (Eucommiaceae)	1						1	1		1					1	1			2			1		
Fagus (Fagaceae)																			1					
Fraxinus (Oleaceae)				1																				
Hedera helix-type (Araliaceae)					1																		2	2
Ilex (Aquifoliaceae)																					1			
Juglans (Juglandaceae)																	1							
Liquidambar (Altingiaceae)	1	1		1	1	2			1	4		3	1	4	1	2	1	3	5	1	1		3	
Myrica (Myricaceae)	4		1	4		3	1	1	2	2		6		2		1	2	4	3	3		2		
Parrotia cf. *persica* (Hamamelidaceae)																1	1							
Parthenocissus cf. *henryana* (Vitaceae)		1	1										6	1	2									1
Platanus (Platanaceae)		1									1						1	2						
Populus (Salicaceae)					1	1	1		2	2		1		2		2				1		1	1	3
Pterocarya (Juglandaceae)	1		1	3		1	3		1	5	1	1	2	1	5	7	4	9	6	1	6	1	3	
Quercus (deciduous-type) (Fagaceae)	3	1	1			3	2	1	1	1	2			1	1	1					3		2	
Salix (Salicaceae)				1										1			1							
Sambucus (Adoxaceae)									1															
*Tamarix** (Tamaricaceae)						1																		
Tilia (Malvaceae)									1	3	1					3	2	1				1	3	9
Ulmus (Ulmaceae)	2	3	6	1	4			5	3	2	2			4	9	11	3	3	9	1		3	5	
Planera-type (Ulmaceae)							1										3					1		
Vitis (Vitaceae)														1				1						
Zelkova (Ulmaceae)		2	7	3	5	5	4	9	6	1	1			3	6	3	7	5	5	1	1		1	5
MESO-MICROTHERMIC TREES																								
Cedrus (Pinaceae)																							1	
Tsuga (Pinaceae)	2						2		1				1					2						
MICROTHERMIC TREES																								
Abies (Pinaceae)	1						4												1	5				
Picea (Pinaceae)	5	2			1	2	11	1			1						1	1				1		

Sample number	GS114	GS115	GS116	GS117	GS118	GS119	GS120	GS121	GS122	GS123	GS124	GS125	GS126	GS127	GS128	GS129	GS130	GS131	GS132	GS133	GS134	GS135	GS136	GS137
TREES (OR SHRUBS) WITHOUT PRECISE ECOLOGICAL SIGNIFICANCE																								
Juniperus-Cupressus-type (Cupressaceae)	1	12	5	2	10	5	2	8	14	10	2	3	7	3	3	1	3	1	1	7	6	2	13	9
*Pinus (*diplostellate-type) (Pinaceae)	26	5	2	22	2	13	88	1	11	10	14	5	2	2	1	3	3	6	3	18	8	2	14	1
*Pinus (*haplostellate-type) (Pinaceae)																	1						3	
Pinus haploxylon-type (Pinaceae)							2												2					
Pinaceae (unidentified pollen grains)	3	1		3			7			1		1					3	1	1	1			1	1
Dicranostyles-type (Convolvulaceae)																				1				
Ranunculaceae	6										3								1		1			
Rhamnaceae									1				1		2									
Rosaceae		3	1			2	1	2	1			2	2	2	1	6	2		4		1	2	1	
Rutaceae												2												1
WATER PLANTS																								
Alismataceae																		1						
Epilobium (Onagraceae)								1	1															
Menyanthaceae	1				1					1			1	2					3					
Onagraceae													1				1	1		1				
Potamogeton (Potamogetonaceae)		1													1								1	
Sparganium (Typhaceae)							1		1										3					
Typha angustifolia-type (Typhaceae)									1															
Typha (Typhaceae)		1		1			2									1		2						
COSMOPOLITAN HERBS AND BUSHES																								
*Ephedra** (Ephedraceae)	1																							
Amaranthaceae*																				1		1		
Aquilegia-type (Ranunculaceae)											2		1								1			
*Artemisia** (Compositae)	4										1				15								1	
Apiaceae																3								
Caryophyllaceae*	1																							
Compositae Asteroideae	5																							
Compositae Cichorioideae	2																							
Convolvulus (Convolvulaceae)									1							1	1	1						
Crassulaceae		1														3								
Cyperaceae	7							1		1		3	1				1		2		1			
Euphorbia (Euphorbiaceae)											1													
cf. Hypericum (Hypericaceae)				1																				
Mercurialis (Euphorbiaceae)																1								
Morina (Caprifoliaceae)																	1							
Nitraria* (Nitrariaceae)															2		1	1					1	
Papaveraceae				1		1						1											1	
Plantago (Plantaginaceae)			1	1																				
Plumbaginaceae*																			1					
Poaceae	22						1									1	1		1				1	
Polygonum aviculare-type (Polygonaceae)															1									
Resedaceae					1	1											1							
Ribes (Grossulariaceae)	1															1								
Rumex (Polygonaceae)															2	1	2	1	1				3	
Saxifragaceae										1														
Scrophulariaceae										2														
Urticaceae						1					1				1			3	1				1	
Total number of identified pollen grains	**133**	**111**	**108**	**136**	**105**	**122**	**188**	**110**	**120**	**123**	**118**	**116**	**117**	**110**	**106**	**108**	**114**	**112**	**115**	**150**	**120**	**105**	**120**	**116**
Unidentified pollen grains		1			1	1			1			1	1			2	1		1				1	1
Indeterminable pollen grains	7	6	17	2	7	5	11	10	2	5	22	4	12	17	6	9	1	7	10	4	25	3	10	6
PTERIDOPHYTES																								
Azolla (Salviniaceae)	8		1						1															
Osmunda (Osmundaceae)		2	1		1		1	6		1	5		1	2		1	1	2	2	3		3	1	1
Polypodiaceae										1														
Selaginella wildenowii-type (Selaginellaceae)				1					3							1				1		1	1	
Selaginella selaginelloides-type (Selaginellaceae)															3									
Unidentified monolete spores	41	7	6	1	4	1	14	7	10	11	11	4	9	19	27	15	23	12	8	6	30	56	22	10
Unidentified trilete spores	32		14	2	4	2	9	5	4	2	5	1		3		5		4	6	1	4		4	2
Unidentified large spores							7		1	1					5		1							
BRYOPHYTES																								
Unidentified spores	5						1																	
OTHER PALYNOMORPHS																								
Botryococcus	X						X	X												X				
Fungi	2					1	1		2	3			3		87	16	67	7	8	1	4	1	4	
Algae	42	10	16	3	3	8	8	9	6	7	7	3	5	5	7	11	6	12	9	4	16	14	11	1
Marine dinoflagellate cysts	5	65		30		110			1	3			1		1		1	1		1			1	
REWORKED PALYNOMORPHS																								
Pollen grains	8	1	0	0		0	2				1			0	1	0	1	6	2	3			1	
Fern spores	6	1	1		1		5		2	3					8	6	6	11	7	2	1	2	15	
Dinoflagellate cysts																	3							

789

790

791 Table DR2. Pollen flora of the Belkovsky Island section. Taxa are organized with respect to
792 their ecological significance. Identification nomenclature: cf., used to reveal which living
793 taxon (species, genus) has the nearest pollen morphology to the fossil pollen within a
794 taxonomic entity (genus, family); -type, used to indicate a pollen-type within a taxonomic
795 entity (genus, family) without a robust significance as identification. Symbols: *, halophyte;
796 X, present.

Sample number	GS07	GS08	GS09	GS10	GS11	GS12	GS13	GS14	GS15	GS16	GS17	GS18	GS19	GS20
Height (m)	0.20	0.30	0.40	0.50	0.60	0.65	0.70	0.75	0.80	1.00	1.20	1.40	1.60	1.80
MEGATHERMIC TREES (OR LIANAS)														
Mimosoideae (Leguminosae)								1						
Canthium-type (Rubiaceae)										1				
MEGA-MESOTHERMIC TREES (OR LIANAS)														
Cathaya (Pinaceae)	5	5	2	5	1		4		3		5	4	2	1
Keteleeria (Pinaceae)					1									2
Sciadopitys (Sciadopytaceae)			1					1						
Glyptostrobus-Taxodium (Cupressaceae)			2	6			1	3		8	4	1	4	
Sequoia-type (Cupressaceae)				5					1	3	5	1	4	
Arecaceae			2	4	1		1	9	4	3	6	4		2
Engelhardia (Juglandaceae)	2	2	4	8	1	4	2	14	1	9	14	5	9	6
Ilex floribunda-type (Aquifoliaceae)											1			
Nyssa (Cornaceae)		1					1							
Platycarya (Juglandaceae)				1										
MESOTHERMIC TREES (OR LIANAS)														
Acer (Sapindaceae)	1		1	1			4	1		1				
Aesculus (Sapindaceae)							1							1
Alnus (Betulaceae)	4	1	8	20	6	4	1	8	4	6	3	5	13	3
Betula-type (Betulaceae)	4	1	4		2	14	14	15	3	6		6	3	9
Corylus-type (Betulaceae)				1			1			1				
Betula (Betulaceae)	14	6	7	8	10	17	18	14	13		8	7	11	10
Buxus sempervirens-type (Buxaceae)			1									1		1
Carpinus (Betulaceae)		1	3	11	6	5	10		3	5	4	1	6	4
Carya (Juglandaceae)				4						2			2	1
Celtis (Cannabaceae)						1		1				2	2	
Decodon (Lythraceae)													1	
Ericaceae	4	3	10	5	5	7	8	4	6	12	5	3	9	4
Eucommia (Eucommiaceae)				1				1						
Fagus (Fagaceae)					1									
Fraxinus (Oleaceae)		1						1	1			1		
Hedera helix-type (Araliaceae)				1										
Juglans (Juglandaceae)			1											1
Lonicera (Caprifoliaceae)			1						1					
Myrica (Myricaceae)		1	4	2	6	11	3	3	4	3	4	2	3	7
Parrotia cf. *persica* (Hamamelidaceae)										1				
Parthenocissus cf. *henryana* (Vitaceae)										1				
Platanus (Platanaceae)													1	
Populus (Salicaceae)	1	1		1	1	2	3	2		2	2		3	2
Pterocarya (Juglandaceae)	1		2	1	2	1		4	1	1	1	1	1	2
Quercus (deciduous-type) (Fagaceae)	1		1			2	2	5	2	2				
Salix (Salicaceae)	2		1	1		2	8		4		1			
Tilia (Malvaceae)		1		1										
Ulmus (Ulmaceae)			2	2				2		1			1	1
Zelkova (Ulmaceae)							1						2	1
MESO-MICROTHERMIC TREES (OR LIANAS)														
Tsuga (Pinaceae)	9	4	7	7	6	2	8	1	2	5	10	7	9	3
MICROTHERMIC TREES (OR LIANAS)														
Abies (Pinaceae)	18	7	8		4	3	2		3	2	2	1	4	3
Larix (Pinaceae)					1									
Picea (Pinaceae)	32	25	25	7	32	5	5	1	31	25	21	30	14	28

797

798

Sample number	GS07	GS08	GS09	GS10	GS11	GS12	GS13	GS14	GS15	GS16	GS17	GS18	GS19	GS20
TREES (OR SHRUBS) WITHOUT PRECISE ECOLOGICAL SIGNIFICANCE														
Juniperus-*Cupressus*-type (Cupressaceae)	1		2	5	4	2	1	3	3	3	4	3	4	10
*Pinus (*diplostellate-type) (Pinaceae)	66	50	101	40	65	22	12	7	55	24	40	52	45	56
*Pinus (*haplostellate-type) (Pinaceae)	2			1							1			1
Pinus haploxylon-type (Pinaceae)	2		1		1			1	1	2	1		2	2
Pinaceae (unidentified pollen grains)	11	5	12	5	7	2	6	2	10	4	4	8	5	9
Ranunculaceae	1		1	1	9	6	1	5	1				2	1
Rosaceae								2		1				1
WATER PLANTS														
Lythrum (Lythraceae)											1			
Lythraceae	1											2		
Menyanthaceae			1	2	1	4			1		1			1
Unidentified aquatic Monocotylédone							1							
Nymphaeaceae						1								
Onagraceae											1			3
Potamogeton (Potamogetonaceae)		1		1		2	1	1				1		1
Restionaceae														1
Ruppia (Ruppiaceae)												1		
Sparganium (Typhaceae)									3			1		2
Typha (Typhaceae)		1		2	1			3		1	4	1	3	
COSMOPOLITAN HERBS AND BUSHES														
Anemone (Ranunculaceae)								3						
Asphodelus (Xanthorrhoeaceae)							1							
Campanulaceae														1
Cannabaceae					1									
Centaurea (Compositae)														1
Cyperaceae	1	1	6		4	6	4		8	2		12	4	3
Dipsacus-type (Caprifoliaceae)										1				
Liliaceae													2	
Phlomis (Lamiaceae)								1						
Plantago (Plantaginaceae)												1		
Polygonum aviculare-type (Polygonaceae)														
Rumex (Polygonaceae)					1									
Spergula (Caryophyllaceae)											1			
Urticaceae				1				1	1				1	
Total number of identified pollen grains	**183**	**118**	**221**	**161**	**180**	**125**	**125**	**120**	**170**	**138**	**154**	**164**	**172**	**185**
Unidentified pollen grains									1	2				
Indeterminable pollen grains			8	2	5	2	8	8	5		8	5	6	4
PTERIDOPHYTES														
Azolla (Salviniaceae)		2		7				14		4	3		2	
Azolla (Salviniaceae) sporangium								3						
Osmunda (Osmundaceae)		1		2			2	1	7	5	3	3	6	5
Polypodiaceae														
Schizaeaceae														
Unidentified monolete spores	58	23	73	61	23	54	77	92	123	63	73	101	48	70
Unidentified trilete spores	25	13	34	13	20	44	71	16	53	14	36	49	14	41
Unidentified large spores		2		1				7		11	2		2	
BRYOPHYTES														
Unidentified spores			2	1			1	3					1	2
OTHER PALYNOMORPHS														
Botryococcus	X			X			X	X		X				X
Fungi			3	2		2	1	1	3	11	6	2	3	4
Algae	19	2	23	21	18	102	156	80	33	10	15	19	15	34
Marine dinoflagellate cysts								1	2					1
REWORKED PALYNOMORPHS														
Pollen grains		5	2	7	1	3				2	1	5	2	5
Fern spores	1	1	7	11		7		1		3	9	1	6	7
Dinoflagellate cysts		1		2										1

Table DR3. Geochemistry, palynofacies, mineralogy and bioclimatic data for the studied Eocene samples of Faddeevsky and Belkovsky islands. Proportions of kaolinite, chlorite, smectite and illite are expressed in % of the clay assemblage; the most likely values of annual temperatures (Ta), coldest month temperatures (Tc) and warmest month temperatures (Tw),

and their minimum (min) and maximum values (max), are expressed in °C; The most likely values of mean annual precipitation (Pa) and their minimum (min) and maximum values (max) are given in mm/year. TOC = Total Organic Carbon; TOC RE6 = Total Organic Carbon contents determined from Rock Eval 6 pyrolysis; TN = Total Nitrogen; TS = Total Sulfur.

lithology	$\delta^{13}C_{TOC}$ (‰ VPDB) sideritе-free	$\delta^{13}C_{TOC}$ (‰ VPDB)	SD $\delta^{13}C_{TOC}$ (‰ VPDB)	TN (wt.%)	SD TN (wt.%)	TOC (wt.%)	SD TOC (wt.%)C	TS (wt.%)	SD TS (wt.%)	C/N (molar ratio)	C/S (molar ratio)	TOC R-E6 (wt.%)	S1 (mgHC/g rock)	S2 (mgHC/g rock)	T_{max} (°C)	HI	OI	A.O.M. (%)	*Botryococcus* (%)	Pollen and spores	Bisaccate pollen(%)	PM3 (%)	PM2 (%)	PM1 (%)	PM4 (%)	Amber (%)	
Sandy clay	-26,48	-26,48	0,58	0,02	0,00	0,15	0,01	0,07	0,04	8,46	5,60	0,22	0,02	0,19	609	86	210	5,5	2,4	2,4	5,0	34,9	20,4	5,1	24,3	0,0
Brown clay	-26,67	-26,67	0,32	0,28	0,21	24,94	0,49	2,37	0,07	104,86	28,11	6,81	0,57	5,71	408	84	74									
Lignite seam	-26,87	-26,87	0,05	0,54	0,42	49,74	0,98	4,66	0,11	108,47	28,44	49,74	10,04	105,11	372	211	54	65,5	4,0	1,0	0,7	4,8	6,9	0,7	0,0	16,4
Brown clay	-25,54	-25,54	0,05	0,57	0,06	32,92	0,71	1,16	0,11	67,37	75,96	12,15	1,62	30,98	426	255	53									
Lignite seam	-25,74	-25,74	0,02	1,26	0,46	62,17	0,52	3,69	0,10	57,79	44,98	47,29	15,31	84,02	364	178	69	54,5	3,5	0,4	1,0	7,9	26,9	0,3	0,0	5,5
Brown clay	-26,07	-26,07	0,04	0,25	0,02	7,07	0,11	3,04	0,07	33,64	6,20	5,97	0,49	5,14	407	86	89									
Lignite seam	-28,45	-28,45	0,08	1,00	0,65	20,38	0,83	2,44	0,52	23,78	22,25	54,71	28,87	238,93	379	437	45	44,6	6,2	2,1	2,9	7,2	23,2	6,3	6,5	1,1
Lignite seam	-26,07	-26,07	0,19	0,97	0,51	17,73	13,07	8,64	1,54	21,32	5,47	17,73	3,37	57,83	426	326	61	60,4	0,0	0,8	1,0	2,1	8,3	0,0	0,0	27,4
Grey clay	-24,56	-24,56	0,06	0,17	0,01	4,58	0,05	0,36	0,00	31,40	34,08	2,3	0,18	2,21	420	96	88	4,2	0,0	5,4	7,8	45,3	34,5	1,2	1,5	0,0
Grey clay	-24,36	-24,36	0,01	0,23	0,03	15,54	0,02	2,58	0,00	78,80	16,06	13,14	1,71	15,17	363	115	59									
Lignite seam	-25,50	-25,50	0,24	0,92	0,52	61,59	1,17	2,25	0,21	78,52	73,12	43,31	18,89	179,83	397	415	49	50,2	0,8	1,7	2,7	2,7	11,0	1,4	2,5	26,9
Grey clay	-24,98	-24,98	0,52	0,15	0,11	11,26	5,69	0,94	0,32	90,56	31,90	10,43	1,16	11,56	353	111	52									
Lignite seam	-26,80	-26,80	0,01	0,73	0,16	62,15	3,95	1,39	0,14	99,33	119,53	49,3	19,11	145,20	362	295	44									
Lignite seam	-26,15	-26,15	0,21	0,71	0,11	64,62	1,34	1,98	0,25	106,94	87,14	47,12	18,35	145,78	398	309	60	75,4	1,0	3,4	5,6	1,2	12,2	0,0	0,0	1,2
Clayey sandstone	-24,90	-24,90	0,08	0,27	0,01	9,28	1,09	0,29	0,03	40,86	84,17	8,93	0,51	8,46	409	95	100									
Clayey sandstone		5,30	0,07	0,07	0,04	4,64	0,35	0,10	0,02	77,33	126,26	1,35	0,02	0,44	391	33	1505	18,0	0,0	3,2	2,5	18,0	46,2	8,7	3,5	0,0
Silty clay		-1,37	0,02	0,08	0,01	4,60	0,08	0,10	0,04	71,48	128,98	1,83	0,04	1,00	424	55	1283	6,9	0,0	2,5	5,6	33,8	38,4	8,4	1,9	2,5
Silty clay	-25,66	-25,66	0,18	0,07	0,01	0,76	0,03	0,06	0,00	13,64	33,22	0,84	0,04	0,43	437	51	514	9,2	0,0	0,6	4,6	42,9	36,2	3,4	2,2	0,0
Silty clay	-26,15	-26,15	0,00	0,09	0,01	0,89	0,04	0,05	0,01	12,22	51,59	3,69	0,74	6,61	418	179	79	9,6	1,0	0,5	2,6	33,2	42,8	6,3	3,9	0,0
Sandy clay	-25,23	-25,23	0,04	0,18	0,02	6,80	0,42	0,46	0,01	45,33	39,55	1,46	0,04	0,59	436	40	906	6,5	1,1	0,3	1,7	23,9	53,5	4,5	1,4	7,0
Lignite seam	-25,79	-25,79	0,09	1,12	0,24	63,81	1,11	1,39	0,01	66,46	122,54	46,55	18,14	166,64	407	358	52	44,4	0,6	0,3	1,9	3,0	28,9	1,3	0,2	19,4
Lignite seam	-27,64	-27,64	0,05	1,30	0,25	57,36	0,92	2,30	0,20	51,68	66,63	46,14	11,44	63,91	394	139	88	55,8	0,0	0,3	2,6	9,1	32,1	0,0	0,0	0,0
Grey clay	-24,82	-24,82	0,08	0,08	0,00	3,33	0,44	0,32	0,02	48,56	28,15	3,73	0,35	3,69	367	99	54	18,1	3,0	0,4	4,5	14,7	51,6	4,3	3,2	0,0
Lignite seam	-26,18	-26,18	0,27	0,62	0,10	31,11	2,21	0,96	0,14	58,53	86,36	50,16	8,46	87,83	428	406	48									
Amber particles		-22,68	0,03	0,44	0,60	82,51	0,02	1,62	0,28	221,28	136,15	72,86			1025											
Unconsolidated sand	-26,57	-26,57	0,15	0,05	0,00	0,435	0,05	0,49	0,06	10,15	2,36	0,25	0,03	0,17	404	70	224	9,3	0,8	6,6	7,5	24,2	47,7	2,7	1,2	0,0
Unconsolidated sand	-26,18	-26,18	0,27	0,04	0,01	0,275	0,01	0,25	0,02	9,17	2,91	0,14	0,02	0,16	382	115	264									
Unconsolidated sand	-26,36	-26,36	0,31	0,06	0,01	0,295	0,01	0,59	0,07	6,26	1,33	0,14	0,02	0,15	391	104	428	12,1	2,4	5,3	6,6	22,6	49,0	1,2	0,8	0,0
Unconsolidated sand	-25,82	-25,82	0,65	0,05	0,01	0,315	0,04	0,50	0,03	8,17	1,67	0,18	0,03	0,13	390	72	314	3,1	2,1	5,4	4,0	29,6	52,0	0,9	1,8	0,0
Unconsolidated sand	-27,09	-27,09	0,01	0,05	0,01	0,585	0,05	0,66	0,04	15,17	2,35	0,32	0,06	0,19	413	59	317	9,5	2,1	8,8	5,5	22,8	46,1	2,7	2,4	0,0
Unconsolidated sand	-27,53	-27,53	0,09	0,26	0,04	6,66	0,91	2,81	0,18	30,47	6,33	6,83	1,03	4,53	385	66	150	14,4	1,5	3,2	3,5	25,3	48,0	3,5	0,6	0,0
Dark grey clay	-27,65	-27,65	0,06	0,44	0,03	16,235	1,11	3,32	0,40	43,05	13,03	12,84	2,87	13,55	397	106	107	25,5	0,0	1,6	6,0	8,1	58,5	0,2	0,0	0,0
Dark grey clay	-27,89	-27,89	0,03	0,55	0,02	14,74	0,18	2,99	0,06	31,55	13,16	13,02	2,78	14,99	407	115	107									
Grey clay	-27,33	-27,33	0,03	0,08	0,01	1,925	0,11	0,99	0,02	29,94	5,19	1,28	0,25	0,73	393	57	145	5,6	3,3	1,4	8,9	53,8	25,2	1,4	0,5	0,0
Grey clay	-26,80	-26,80	0,02	0,12	0,01	2,555	0,23	1,03	0,04	25,92	6,61	1,88	0,33	0,93	402	49	142									
Grey clay	-26,64	-26,64	0,14	0,06	0,01	0,83	0,07	0,36	0,03	16,14	6,14	1,14	0,15	0,52	403	45	140									
Grey clay	-26,89	-26,89	0,09	0,07	0,01	1,285	0,04	0,54	0,01	21,42	6,37	0,7	0,07	0,23	399	33	189	12,2	1,6	2,9	7,0	46,3	26,0	2,8	1,1	0,0
Grey clay	-26,73	-26,73	0,09	0,11	0,02	2,07	0,03	1,78	0,01	23,00	3,11	1,16	0,17	0,41	407	36	209									
Clay with boulders	-26,76	-26,76	0,02	0,04	0,01	0,41	0,01	2,36	0,14	13,67	0,46	0,24	0,02	0,08	406	33	296	9,2	1,1	1,2	7,6	48,0	28,3	3,1	1,5	0,0
Sandy clay	-25,57	-25,57	0,57	0,02	0,00	0,185	0,04	0,13	0,02	10,79	3,70	0,12	0,02	0,07	399	62	248	4,0	0,9	9,4	7,7	27,5	45,9	1,6	2,4	0,0
Sandy clay	-25,91	-25,91	0,67	0,04	0,01	0,315	0,12	0,39	0,15	10,50	2,14	0,22	0,03	0,10	404	45	238	7,25	1,09	5,80	2,36	32,61	46,20	3,44	1,27	0

	Height (m)	Clay (%)	Quartz (%)	Orthoclase (%)	Albite (%)	Jarosite (%)	Siderite (%)	Pyrite (%)	Smectite (001)	Illite (001)	Kaolinite (001)	Chlorite (001)	Ta min	Ta	Ta max	Tc min	Tc	Tc max	Tw min	Tw	Tw max	Pa min	Pa	Pa max
Faddeevsky																								
GS114	1,05	30,07	51,02	7,20	11,68	0,03	0,00	0,00	5,06	35,62	52,85	6,48	10,0	15,8	22,0	0,0	6,4	15,0	22,5	24,8	28,0	1000	1135	1300
GS115	1,80	56,87	34,52	0,00	1,80	1,75	0,00	5,07	0,00	62,22	10,45	27,33	16,0	18,7	22,0	10,0	10,5	12,0	25,0	26,5	28,0	1100	1273	1400
GS116	1,95	55,22	40,25	0,57	1,00	0,74	0,00	2,21	1,01	43,05	38,24	17,69	16,0	18,2	22,0	5,0	10,4	15,0	25,0	26,2	28,0	1100	1256	1400
GS117	2,05	54,00	44,50	0,99	0,41	0,00	0,00	0,09	1,70	28,79	60,87	8,65	16,0	18,6	22,0	10,0	10,5	15,5	25,0	26,5	28,0	1100	1262	1400
GS118	2,45	56,54	38,95	0,54	0,97	1,58	0,00	1,42	2,81	29,74	58,62	8,84	16,0	18,0	22,0	5,0	7,5	11,0	25,0	26,0	28,0	1100	1252	1400
GS119	2,75	59,59	32,28	0,00	1,65	3,47	0,00	3,02	4,01	30,78	56,18	9,03	16,0	21,3	23,0	13,0	13,8	15,5	25,0	27,6	28,0	1100	1271	1400
GS120	3,20	58,52	35,72	0,49	1,40	2,01	0,00	1,86	2,45	32,85	55,97	8,73	16,0	18,2	22,0	5,0	7,5	11,0	25,0	26,1	27,8	1100	1256	1400
GS121	3,85	57,25	39,82	1,08	1,10	0,27	0,00	0,48	0,50	35,42	55,73	8,34	16,0	18,3	22,0	5,0	10,4	15,0	25,0	26,2	28,0	1100	1259	1400
GS122	4,15	51,52	45,06	0,97	1,97	0,48	0,00	0,00	7,43	30,55	53,86	8,17	16,0	18,3	22,0	10,0	10,4	12,0	25,0	26,0	27,0	1100	1211	1300
GS123	4,55	65,46	28,93	0,00	0,00	1,93	0,28	3,40	1,36	24,64	64,91	9,09	16,0	18,3	22,0	10,0	10,4	15,0	25,0	26,3	28,0	1100	1265	1400
GS124	5,00	50,76	45,30	0,37	0,38	1,10	0,14	1,94	1,05	32,06	57,81	9,08	16,0	21,3	22,0	13,0	13,8	15,0	25,0	27,7	30,0	900	1154	1400
GS125	5,50	34,62	62,84	0,00	0,86	1,68	0,00	0,00	0,43	47,34	42,89	9,34	16,0	18,9	23,0	10,0	11,2	13,0	25,0	26,4	28,0	1100	1363	1580
GS126	6,10	56,03	39,88	3,06	0,00	1,03	0,00	0,00	0,00	35,88	17,87	46,25	16,0	18,7	22,0	10,0	11,0	12,0	25,0	26,0	27,0	1100	1368	1580
GS127	6,50	36,68	60,31	1,58	0,00	1,42	0,00	0,00	0,07	38,43	38,01	23,49	16,0	21,3	22,0	13,0	13,6	15,0	25,0	27,7	30,0	1100	1269	1400
GS128	7,00	30,59	41,25	2,22	14,44	0,00	11,51	0,00	0,08	38,71	40,22	20,99	18,0	19,5	22,0	10,0	12,4	15,0	25,0	25,9	27,0	1100	1268	1400
GS129	7,60	13,28	35,02	5,88	24,41	0,00	21,41	0,00	0,00	55,99	33,82	10,19	16,0	17,8	20,0	10,0	10,4	15,0	25,0	26,5	28,0	1100	1251	1400
GS130	8,30	25,87	28,88	1,80	8,64	0,00	34,81	0,00	0,00	50,51	33,44	16,05	18,0	21,3	22,0	10,0	10,4	12,0	25,0	27,6	28,0	1100	1210	1300
GS131	18,45	27,12	52,64	11,67	7,82	0,00	0,76	0,00	1,17	45,72	34,81	18,30	18,0	21,3	22,0	10,0	10,4	13,0	25,0	27,7	30,0	1100	1263	1400
GS132	23,60	40,92	43,74	2,57	10,49	0,00	2,27	0,00	2,85	45,61	36,45	15,09	16,0	21,3	22,0	10,0	10,4	13,0	25,0	27,7	28,5	1100	1214	1300
GS133	29,50	47,17	47,11	1,54	3,72	0,28	0,00	0,18	2,15	39,14	46,36	12,36	16,0	18,5	22,0	10,0	10,4	15,5	25,0	26,4	28,0	1100	1268	1400
GS134	30,80	47,59	48,36	1,18	2,55	0,22	0,00	0,10	3,04	36,46	50,47	10,04	16,0	21,3	23,0	10,0	10,4	13,0	25,0	27,6	28,0	1100	1260	1400
GS135	31,75	47,89	49,26	0,92	1,72	0,18	0,00	0,04	3,66	34,59	53,29	8,46	16,0	18,5	22,0	10,0	11,8	15,0	25,0	26,5	28,0	1100	1336	1580
GS136	32,70	48,11	49,93	0,72	1,09	0,15	0,00	0,00	4,13	33,21	55,35	7,31	18,0	21,3	22,0	13,0	13,6	15,0	25,0	27,6	28,0	1000	1157	1300
GS137	35,00	57,14	42,35	0,00	0,00	0,00	0,00	0,51	22,74	18,92	54,14	4,19	16,0	21,3	25,0	5,0	10,4	13,0	25,0	27,7	30,0	1100	1264	1400
GS138 (amber)	-	-	-	-	-	-	-	-	-	-	-	-												
Belkovsky																								
GS07	0,2	4,78	66,05	3,87	23,02	2,28	0	0,00	0,00	52,25	27,86	19,90	10,0	17,5	25,0				22,5	25,3	28,0	600	975	1300
GS08	0,3	8,55	69,00	2,57	18,35	1,53	0	0,00	0,24	47,36	15,87	36,53												
GS09	0,4	7,05	62,12	7,12	21,96	1,76	0	0,00	2,66	59,66	9,90	27,78	16,0	18,5	22,0	5,0	9,0	15,0	25,0	26,2	28,0	1100	1198	1300
GS10	0,5	10,39	62,26	6,30	19,50	1,55	0	0,00	0,00	60,27	10,76	28,97	16,0	18,4	22,0	10,0	11,7	15,0	25,0	25,9	27,0	800	1111	1300
GS11	0,6	5,33	66,24	4,01	21,09	3,33	0	0,00	2,61	48,23	14,92	34,25	16,0	18,8	23,0	5,0	5,5	10,0	22,5	24,6	27,0	600	1054	1300
GS12	0,65	9,62	65,37	2,61	19,07	3,33	0	0,00	0,00	74,16	23,57	2,27	15,0	18,1	25,0	10,0	11,7	15,5	25,0	25,8	27,0	800	986	1100
GS13	0,7	9,21	58,79	5,75	15,47	10,77	0	0,00	0,00	52,46	44,53	3,01	16,0	18,7	22,0	5,0	10,4	13,0	25,0	25,9	27,0	900	1111	1300
GS14	0,75	6,75	64,18	2,47	17,06	9,55	0	0,00	0,56	58,15	41,29	0,00	16,0	18,6	22,0	10,0	11,7	15,0	25,0	26,2	27,8	1100	1342	1580
GS15	0,8	5,44	59,30	6,37	25,76	2,67	0	0,46	0,00	64,63	0,00	35,37	15,0	18,7	25,0	5,0	9,1	15,5	22,5	25,2	28,0	600	1036	1300
GS16	1	10,03	67,14	1,22	18,22	3,39	0	0,00	0,00	57,30	16,12	26,58	16,0	18,1	20,0	5,0	5,6	8,0	25,0	26,1	27,0	800	1087	1300
GS17	1,2	17,34	61,29	4,63	14,83	1,92	0	0,00	0,00	56,20	16,56	27,25	16,0	19,3	25,0	10,0	12,1	15,5	25,0	26,4	28,0	1100	1205	1300
GS18	1,4	7,22	66,99	3,59	19,69	2,31	0	0,21	0,00	59,52	4,56	35,92	16,0	19,3	25,0	10,0	12,1	15,5	25,0	26,4	27,8	1100	1212	1300
GS19	1,6	12,53	60,90	2,37	14,68	9,52	0	0,00	2,42	52,85	24,18	20,55	16,0	18,3	22,0	5,0	10,4	15,5	25,0	25,9	27,0	800	1086	1300
GS20	1,8	12,46	71,84	5,67	5,25	3,88	0	0,90	0,18	31,88	0,00	67,94	16,0	18,7	22,0	6,4	8,8	11,0	25,0	26,2	28,0	1000	1153	1300
GS21	2	17,13	60,76	7,57	14,29	0,24	0	0,00	0,00	46,78	18,76	34,47												
GS22	2,2	10,50	60,90	3,19	24,24	1,17	0	0,00	0,00	56,05	12,03	31,92												

828 Table DR4. Determination coefficients, sign of the slope and *p*-values obtained by linear
829 correlation between the carbon isotope composition of siderite-free, total organic matter
830 ($\delta^{13}C_{TOC}$) and the palynofacies and geochemical parameters. Only values highlighted in gray
831 are considered highly significant (*p*-values<0.05). Abbreviations: AOM = Amorphous
832 Organic Matter; TOC = Total Organic Carbon; PM = Palynomacerals; HI = Hydrogen Index;
833 OI = Oxygen Index.
834

	Faddeevsky Island			**Belkovsky Island**		
Variable	R^2	Slope	*p*-value	R^2	Slope	*p*-value
TOC	0.11	–	0.13	0.55	–	1.06E–03
Log TOC	0.04	–	0.36	0.79	–	4.56E–06
C/N (molar ratio)	<0.01	+	0.97	0.71	–	4.03E–05
C/S (molar ratio)	<0.01	–	0.87	0.51	–	1.95E–03
HI (mg HC/gTOC)	0.17	–	0.05	0.04	–	0.48
OI	0.03	+	0.46	0.36	+	0.01
Tmax	<0.01	–	0.75	0.02	–	0.57
AOM (%)	0.19	–	0.12	0.48	–	0.02
Botryococcus (%)	0.24	–	0.08	<0.01	–	0.92
Pollen and spores	0.02	+	0.62	0.38	+	0.04
Bisaccate pollen (%)	0.11	+	0.24	0.02	–	0.65
PM3 (%)	0.13	+	0.20	<0.01	+	0.91
PM1+2 (%)	0.11	+	0.24	<0.01	+	0.66
PM4 (%)	0.03	–	0.54	0.37	+	0.05
Amber (%)	0.01	+	0.74	N/A	N/A	N/A
Botryococcus +AOM+amber	0.12	–	0.22	0.56	–	8.18E–03

835
836

Figure DR1. Location of the study sites. **a**, Position of the New Siberian Islands relative to modern Arctic geography (gray) and its reconstructed position relative to the Eocene North Magnetic Pole (black; see text for explanations). **b**, Simplified geological map of the New Siberian Islands and location of the successions of the Belkovsky (1) and Faddeevsky (2) islands (modified after (Kos'ko and Trufanov, 2002).

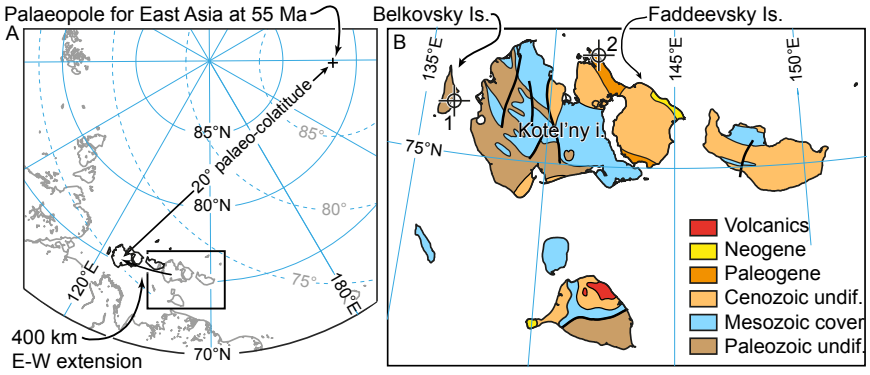

Figure DR2. Exposures of Eocene coastal plain sediments in the New Siberian Islands. **a-b**, Faddeevsky Island; **a**, Basal part of the section (Unit If and base of Unit IIf) showing lignite seams interbedded with brown mudstone beds that infill shallow channels and are overlain by gray sandy claystone beds; **b**, Upper part of the section (Unit IIf and base of Unit IIIf) showing more expanded, gray silty to sandy clays and thinner coal seams; **C,** Top of the section (Unit IIIf) at 34 m showing a dense network of vertical, thin root traces resembling pneumatophores. **d,** Close-up view of basal lignite seams of Unit If showing abundant amber particles within horizontal and flattened tree remains; **e-h**, Belkovsky Island; **e,** General view of the exposure and the measured succession (white arrow) and position of the conglomerate bed (dashed line); **f,** General view of the exposure and measured succession (white arrow) looking to the SE ; **g,** Close-up view of the pebble bed of Unit IIb at 1.8 m; **h,** photograph of

the exposure studied by ref (Kuzmichev et al., 2013) suggesting that the here defined Unit I and II respectively correspond to their bed 10 and 11.

Figure DR3. Geochemistry, palynofacies, and mineralogy of Eocene strata of Faddeevsky and Belkovsky islands. **a**, Rock-Eval pyrolysis; **b**, isotope and elemental geochemistry; **c,** palynofacies; **d,** whole-rock mineralogy deduced from whole-rock DRX data; **e,** clay mineralogy deduced from DRX data.

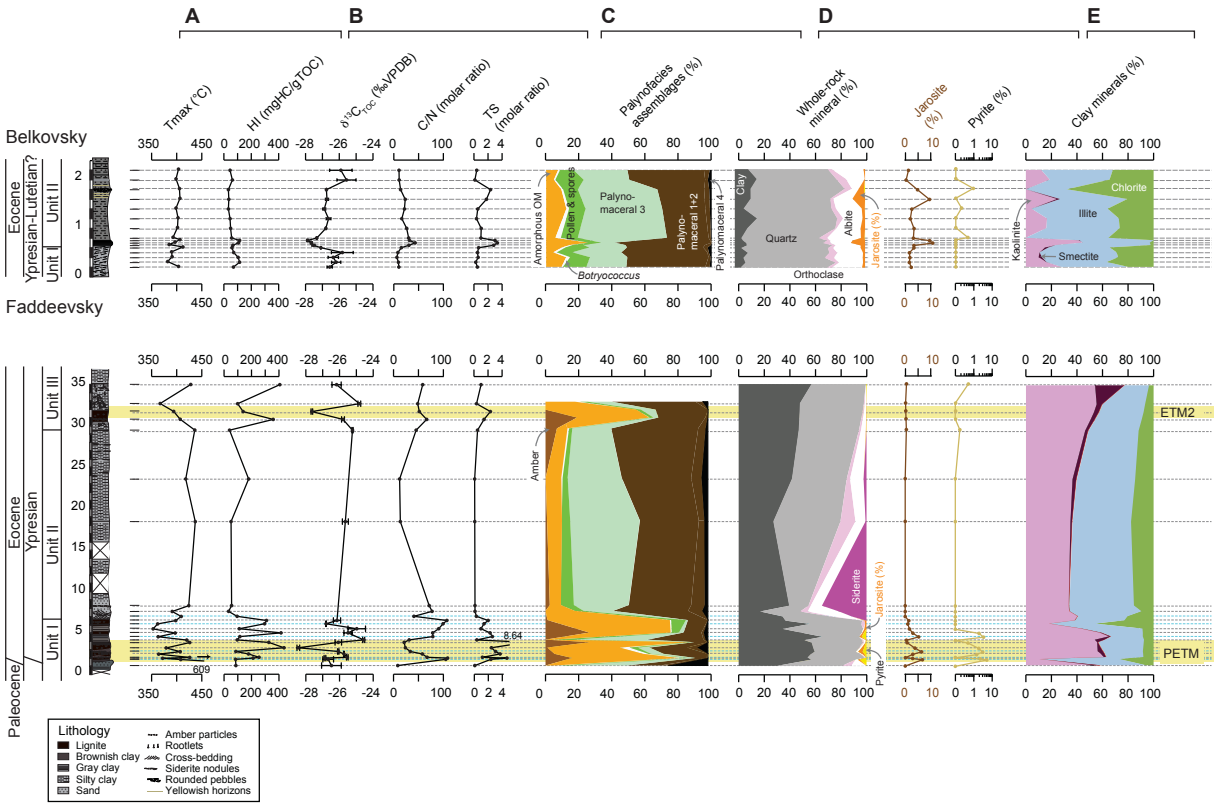

Figure DR4. Specimens of *Apectodinium parvum* from the Faddeevsky Island succession (sample GS119, 2.75 m). **a**, Numerous specimens in a microscope field at x200 magnification in fluorescent light; scale bar = 50 µm. **b,** Specimen in lateral view (b1, in light microscopy; b2, in fluorescence microscopy); scale bar = 10 µm. **c,** Specimen in ventral view (c1, in light microscopy; c2, in fluorescence microscopy); scale bar = 10 µm.

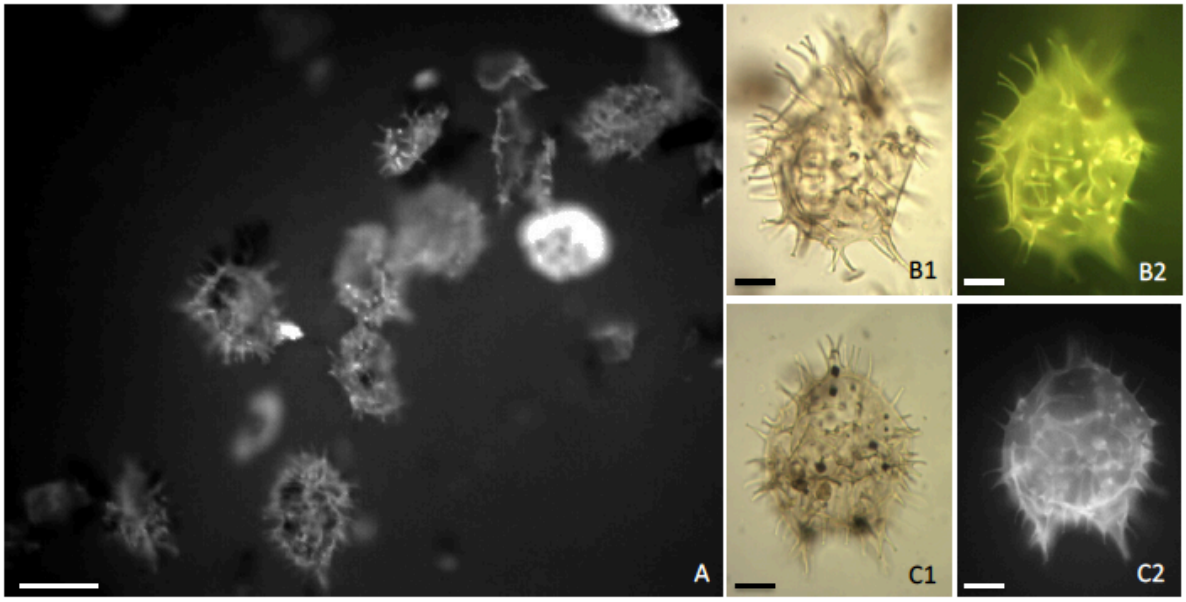

Figure DR5. Chronostratigraphy of the Faddeevsky Island succession. Marine oxygen **a**, and carbon **b**, isotope records for the Paleogene (Vandenberghe et al., 2012). **c,** Close up view (Kirtland Turner et al., 2014) of the Early Eocene carbon isotope record showing the recurrence of negative carbon isotope excursions (note that this curve is based on a slightly different calibration of the absolute timescale). **d,** Organic carbon isotope record from Faddeevsky Island. The green band shows the preferred correlation of the Faddeevsky section with calibrated marine records.

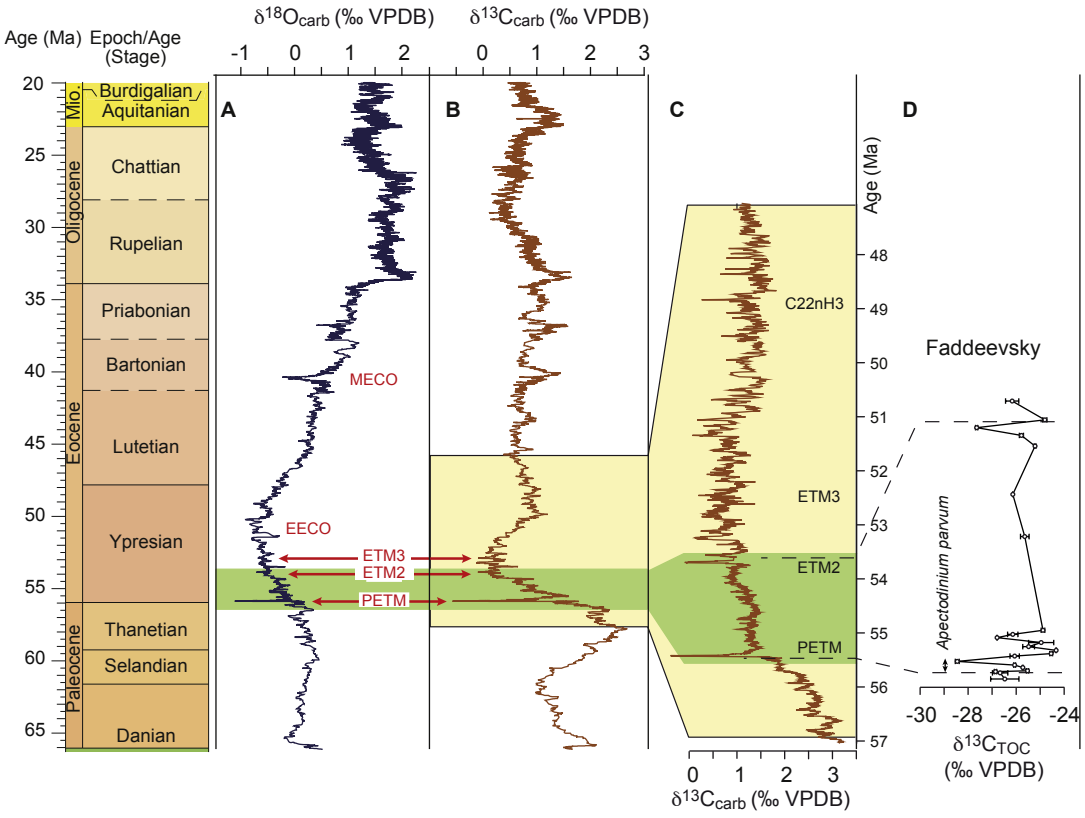

Figure DR6. Comparisons between *Avicennia* pollen grains from the Faddeevsky Island section and modern species. (**a–i**) *Avicennia* (Acanthaceae, Angiosperms) pollen grains from the Faddeevsky Island section: (a–e) at light microscope (scale bar = 10 µm); (a–c), sample GS131 – equatorial view (a, surface of the reticulum constituting the exine ornamentation; b, base of the reticulum; c, optical section and colpi); d–e, sample GS127 – polar view (d,

surface of the reticulum; e, base of the reticulum, optical section and polar triangle); F–I, at scanning electronic microscope (scale bar = 1 µm), sample GS127: f, equatorial view; g, surface of the reticulum of the same grain; h, equatorial view of another grain; I, polar triangle of the same grain; (**j–y**), *Avicennia* (Acanthaceae, Angiosperms) pollen grains from some present-day species: j–p, *A. officinalis* L. (Lyon Herbarium n° 18272); j–n, at light microscope (scale bar = 10 µm); j–k, equatorial view (j, surface and base of the reticulum; k, optical section and colpi); l–n, polar view (l, surface of the reticulum and polar triangle; m, base of the reticulum and polar triangle; n, optical section); (o–p), at scanning electronic microscope (scale bar = 1 µm): o, equatorial view; p, surface of the reticulum of the same grain; q–w, *A. nitida* Jacq. (= *A. germinans* (L.) L.) (Lyon Herbarium n° 312): q–u, at light microscope (scale bar = 10 µm): q–r, equatorial view (q, surface of the reticulum; r, base of the reticulum); s–u, polar view (s, surface of the reticulum and polar triangle; t, base of the reticulum and polar triangle; u, optical section); v–w, at scanning electronic microscope (scale bar = 1 µm): v, polar view; w, surface of the reticulum and polar triangle of the same grain; x–y, *A. tomentosa* Jacq. (= *A. germinans* (L.) L.) (Lyon Herbarium n° 5), at scanning electronic microscope (scale bar = 1 µm): x, equatorial view; y, polar view and polar triangle.

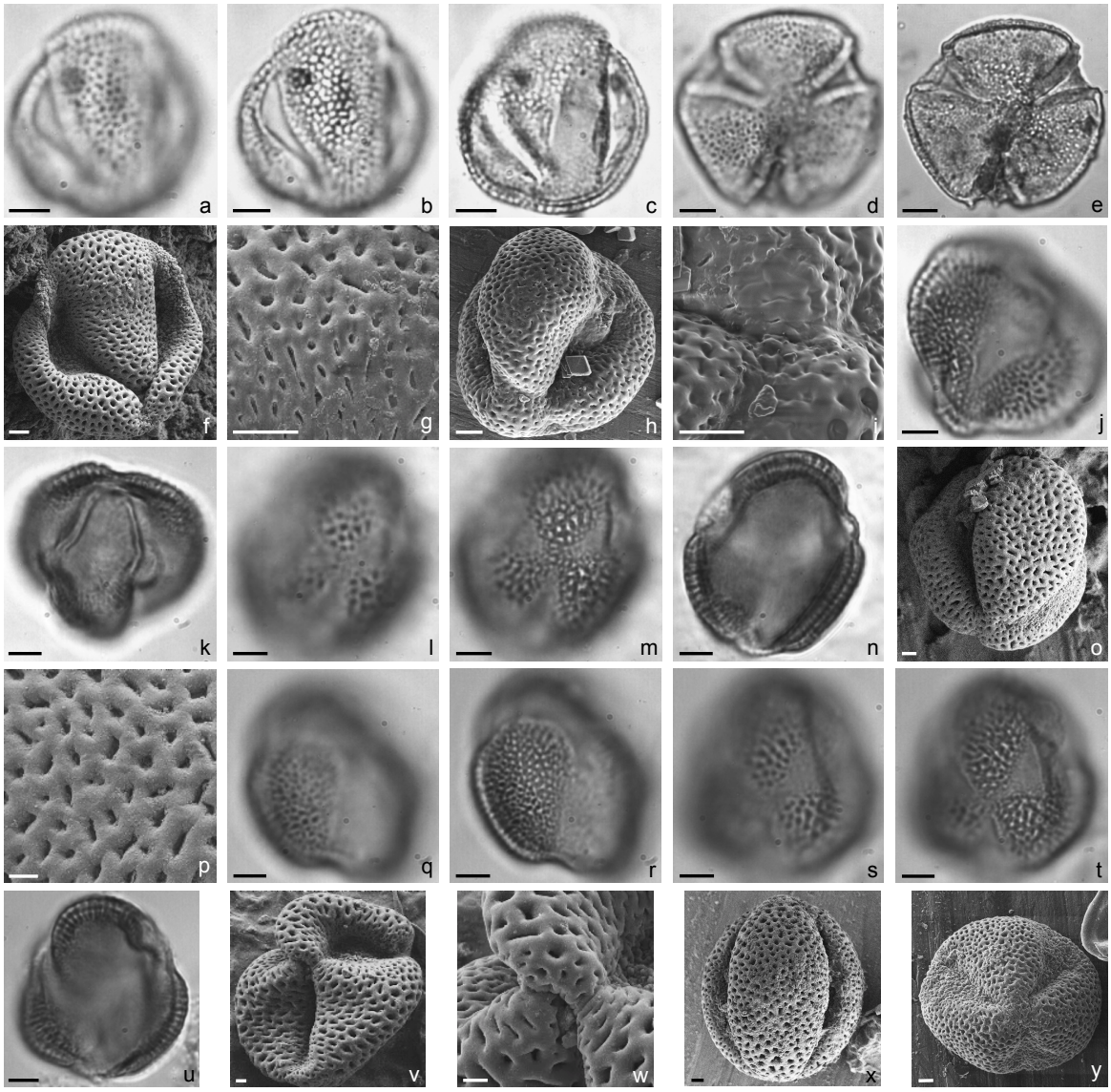

Figure DR7. Organic matter types of Belkovsky and Faddeevsky islands. Plot of hydrogen and oxygen indices obtained from Rock-Eval pyrolysis.